Review

Journal of Biomedical Nanotechnology
Vol. 10, 2921–2949, 2014
www.aspbs.com/jbn

Multifunctional Magnetoplasmonic Nanomaterials and Their Biomedical Applications

Hongjian Zhou[1], Fengming Zou[2], Kwangnak Koh[2], and Jaebeom Lee[1,*]

[1] *Department of Cogno-Mechatronics Engineering, Pusan National University, Busan 609-735, Republic of Korea*
[2] *Department of Nano Fusion Technology, Pusan National University, Miryang 627-706, Republic of Korea*

Multifunctional magnetoplasmonic (Au–Fe_xO_y) nanomaterials are characterized by some features of iron oxide and gold, such as surface chemistry, special optical properties, and superparamagnetic properties, which have helped to draw much attention to their biomedical applications. In this review, the state of the art of this rapidly developing field is described. We review the developments in different approaches to integrating the magnetic and plasmonic properties in a single nanoparticle with different morphological traits. Specific plasmonic and magneto-optical properties of magnetoplasmonic nanoparticles are explained; this information should shed light on the future development of multifunctional magnetoplasmonic nanomaterials. We also review cytotoxicity of magnetoplasmonic nanoparticles by *in vitro* and *in vivo* studies. With the multifunctional properties of magnetoplasmonic nanomaterials, a variety of applications such as biosensor, bioseparation, multimodal imaging, and therapeutics is possible and is highlighted here, in addition to outlining the future trends and perspectives of these sophisticated nanocomposites.

KEYWORDS: *Multifunctional Nanoparticles, Magnetoplasmonic Nanomaterials, Au–Fe_xO_y, Composite Nanoparticles, Biomedical Applications.*

CONTENTS

*Author to whom correspondence should be addressed.
Email: jaebeom@pusan.ac.kr
Received: 15 January 2014
Accepted: 18 February 2014

INTRODUCTION

The interdisciplinary integration of various research fields such as materials science, electronics, and biomedicine with nanotechnology was accelerated by general curiosity and promising applications.[1–4] Such convergence may lead to commercial products in such areas as electronics, high-density memory, sensors, and drug delivery, where nanoparticles (NPs) of multiple components can serve as building blocks to achieve multifunctionality. That is quite fascinating. Therefore, multifunctional nanomaterials have attracted significant interest for biomedical applications such as multimodal imaging,[5–8] gene expression regulation,[9,10] drug delivery,[11,12] and anticancer therapy.[13] Composite NPs containing 2 or more particles of different functionalities represent a fundamental type of a multifunctional nanoscale system.[14] Multifunctional NPs possessing fluorescent, surface plasmon resonant, and/or magnetic properties have been reported. These NPs are synthesized either via direct growth of heterogeneous nanostructures (core–shell[15–17] or heterodimer[18]) or by

enclosing 2 or more types of NPs within a single particle using a coating (e.g., SiO_2[19]).

This technology—combination of NPs of multiple constituents—can also be conducive to diverse, benign multifunctioning.[20, 21] Because of the rapid development of their controlled synthesis, assembly, and modifications, nanomaterials hold great promise in a wide range of biomedical applications.[22–24] There are two kinds of materials that have been extensively exploited since the first chemical synthesis of monodispersed NPs. On the one hand, gold NPs have been widely used in cellular optical imaging, hyperthermia, and sensitive biodetection of DNA and proteins.[13, 25–27] This is because their facile and robust interaction with thiol and disulfide groups enables functionalization of these gold particles with various molecules that are capable of specifically recognizing biological substances; in addition, the diversity of possible practical applications is due to gold NPs'

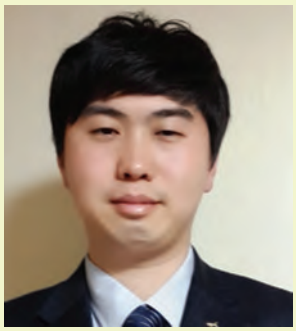

Hongjian Zhou received his B.S. degree in chemistry in 2007 from Nanyang Institute of Technology, China, and M.S. degree in Materials physics and chemistry in 2010 from Jiangsu University of Science and Technology, China. He got his Ph.D. degree in Nano Fusion Technology in 2014 from Pusan National University. Now he is the post-doctoral researcher in Department of Cogno-Mechatronics Engineering, Pusan National University. His current research interest includes synthesis of multi-functional nanoparticles and biomedical applications. He is also interested in surface modification of nanocomposites for biocompatibility and biodegradability in bio-nano-medical applications.

Fengming Zou received her B.S. degree in Bioengineering in 2007 from Chongqing Technology and Business University, China and M.S. degree in 2010 in Biochemistry and Molecular Biology from Jiangsu University of Science and Technology, China. She got her Ph.D. degree in 2013 in Medical Bioscience from Dong-A University, Korea. Now she is the post-doctoral researcher in Department of Nano Fusion Technology, Pusan National University. She is interested in the applications of nanomaterials in biomedical field, such as biosensor, nanoparticles cytotoxicity *in vivo* and *in vitro*, drug delivery etc.

Kwangnak Koh is currently professor in Department of Nano Fusion Technology, Pusan National University, Busan, Korea. He received M.S. degree in 1992 from Pusan National University and Ph.D. degree in 1995 in supramolecular engineering from Kyushu University, Japan. His research interests include biochip, supramolecular engineering, bioanalytical nanochemistry and bionanomaterials.

Jaebeom Lee is currently associate professor in Department of Cogno-Mechatronics Engineering, and Cogno Mechatronics Engineering, Pusan National University, Busan, Korea. He received his B.S. degree in chemistry from Chungnam National University in 1998, and Ph.D. degree in chemistry from the Robert Gordon University, United Kingdom in 2003, and worked as a Research Fellow in Chemical Engineering Department at the University of Michigan, Ann Arbor, USA. Dr. Lee is interested in fabrication and characterization of engineered assemblies of nanomaterials such as semiconductor materials and metallic materials.

exceptional optical properties that are influenced remarkably by their chemical environment, aggregation, the type of particles, and even their conformational differences.[28–32] Moreover, the plasmon resonance peak of Au could be shifted to the near-infrared (NIR) region by changing the proximity and geometry of the Au NPs. On the other hand, magnetic NPs, particularly iron and iron oxide particles including magnetite (Fe_3O_4) and its oxidized form maghemite (γ-Fe_2O_3), have been comprehensively studied for a range of biomedical applications such as hyperthermia treatment of malignant cells, drug delivery, biosensors, enhancement of contrast of magnetic resonance imaging (MRI), magnetic separation, and cell sorting, owing to their unique magnetic properties and biocompatibility.[33–35] Magnetic NPs as special biomolecular carriers (via a suitable immobilization process) hold promise as effective sensors and have been used in immunoassays and in various reactions involving enzymes, proteins, and DNA for magnetically controlled transport and targeted delivery of anticancer drugs.[36, 37] Their tiny size and ability to be transported within biological systems and reactive media is an advantage over conventional support systems.

Hence, if magnetic particles are provided with a gold structure, then the combined benefits of the robust chemistry of a gold surface and the uniqueness of magnetic NPs could be implemented; in addition, the magnetic core could be protected from oxidation and corrosion.[38] Meanwhile, gold has become a popular combining material not only because of its easy reductive preparation, high chemical stability, and biocompatibility, but also owing to its plasmon-derived optical resonance in the visible and NIR region. Furthermore, the gold coating could provide a platform for optical absorption and emission mediated by the collective electronic response of the metal to light; the gold surface could also make these properties compatible with and adaptable to sensor technologies. It is worth noting that besides the separate magnetic and plasmonic properties of hybrid structures discussed in the current article, an interplay, called *magnetoplasmonics*, exists between these 2 properties.

As a form of multifunctional magnetoplasmonic (MFMP) nanomaterials, NPs combining gold and magnetic materials inherit from the 2 components excellent surface chemistry, special optical properties, and superparamagnetic properties, all of which would greatly enhance the potential and broaden the practical applications of such nanomaterials. Accordingly, successful MFMP nanomaterials have been developed for biomedical applications.[39] The magnetic core forms the basis of a particle and allows for a small size with significant magnetic moment. In addition, the MFMP nanocomplex can serve as a good platform for further conjugation of biomolecules. This approach opens up a new avenue for biomedical applications of advanced multifunctional nanomaterials.

Over the past few years, MFMP NPs, such as Au–Fe_3O_4 and γ-Au–Fe_2O_3, have attracted broad attention due to the low reactivity, high chemical stability, biocompatibility, and good affinity of the outer Au layer for amine ($–NH_2$) and thiol (–SH) terminal groups. These particles consisting of a magnetic core with a plasmonic shell have been largely used in the fields of protein separation,[24, 40, 41] drug delivery,[42] cell separation,[43] catalysis,[44] detection,[45] biological sensing and probing,[46] and targeted photothermal (PT) therapy.[47] In particular, in PT therapy, where Au NPs become attached to target cells, the absorbed light energy is quickly transformed into heat and eventually leads to irreparable damage to the target through thermal denaturation and coagulation or through mechanical stress caused by sudden bubble formation.[48] The combination of targeted delivery, improved MRI diagnosis, and NIR photothermal ablation are expected to increase treatment efficacy and to simultaneously minimize the damage to healthy cells and tissues.

Several reviews of magnetoplasmonic nanomaterials were published in recent years. For example, Zhou et al.[49] reviewed core–shell structures—with iron oxide nanoparticles as the core and covalently grafted organic polymers as the shell—as well as the relevant biomedical applications. Wang and colleagues[50] reviewed the synthesis of gold-coated magnetic oxide core@shell NPs, including their synthesis and characterization as well as biological and catalytic applications. Sun and coworkers[51, 52] wrote a good primer on the synthesis methods, properties, and potential applications of multicomponent magnetic NPs. Leung et al.[53] provided an overview of current research

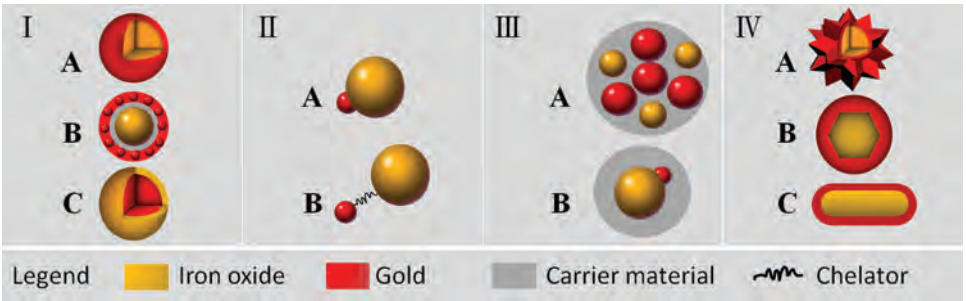

Figure 1. **Schematic representation of four types of MFMP NPs: Type I, Spherical core–shell and core-satellite; Type II, Heterodimer; Type III, Multicomponent hybrid, Type IV, Non-spherical core–shell.**

activities with the focus on the synthesis and practical applications of gold and iron oxide hybrid nanocomposite materials. After reviewing these articles, to avoid any redundancy, we focus here on the current status of biomedical applications of MFMP nanomaterials. Including the introduction, this article contains 6 sections. In the second section, the synthesis of MFMP NPs with varied morphology is introduced, which includes spherical core–shell, core-satellite, heterodimer, multicomponent hybrid, and nonspherical core–shell architectures. The schematic representation of 4 types of magnetoplasmonic nanoparticles is shown in Figure 1. The third section discusses enhanced plasmonic and magneto-optical properties of MFMP NPs. The fourth section reviews the cytotoxicity of MFMP NPs in *in vitro* and *in vivo* studies. The fifth section introduces the proper design of magnetoplasmonic NPs for different biomedical applications, which include several types of biosensors, bioseparation, multimodal imaging, and therapeutics. Finally, in the sixth section, we provide a summary and our own perspectives on this active area of research.

STRUCTURE AND SYNTHESIS OF MAGNETOPLASMONIC NANOPARTICLES

MFMP NPs are an attractive composite system:[54–56] with Au and magnetic components, especially high-moment metallic magnetic components, NPs can be stabilized more efficiently in corrosive biological conditions and be readily functionalized thanks to the well-developed Au–S chemistry; gold also imparts plasmonic properties to the magnetic NPs. This design makes the magnetoplasmonic composite NPs an interesting candidate for magnetic, optical, and biomedical applications.

Several approaches for the preparation of MFMP NPs with varied multiform morphological traits (spherical core–shell, core-satellite, heterodimer, multicomponent hybrid, and nonspherical core–shell architectures) have been reported in the literature, including reactions involving laser ablation,[57] layer-by-layer electrostatic deposition,[58] redox transmetalation,[59] the reverse-micelle method,[60] microemulsion,[56] ray radiation, sonochemical reaction, and chemical reduction in aqueous and organic phases, among others. In any case, synthesizing MFMP NPs is a challenge due to the difference in surface energies of the 2 materials;[61] this difference commonly leads to the segregation of the gold and magnetic components of NPs.

Spherical Core–Shell and Core-Satellite Nanoparticles (Type I)

This section discusses NPs that resemble the structure denoted as Type I in Figure 1, in which the magnetic material (Fe_xO_y) and gold (Au) are fused together to form either a core–shell or a core-satellite nanostructure. Despite the generally large lattice mismatch between magnetic and gold nanocrystals, it has recently been shown that it is possible to combine the 2 materials within 1 nanocrystal, although the mechanism of attachment has not been fully elucidated yet. The several examples discussed below all involve synthesis using a chemical procedure, in which the core is synthesized prior to the attachment of the shell.

Core–shell nanostructures have stimulated great interest in the past decades because of their enhanced optical and tunable surface properties, electronic and catalytic properties, and the consequent wide range of potential applications.[62–65] Generally, the shell layer coating the core can protect the core from oxidation and enhance its stability and biocompatibility; the outer layer materials may also provide a platform for surface modifications and functionalization and even provide a natural vehicle for construction of hybrid multifunctional materials.[66] Moreover, the physical and chemical properties of the core–shell nanostructures can be tailored conveniently by controlling their composition and the relative size of the core to shell. Three spherical core–shell structures of magnetoplasmonic nanoparticles have been successfully synthesized: Fe_xO_y@Au core–shell, Fe_xO_y@Au core-satellite, and Au@Fe_xO_y core–shell structures (Type I in Fig. 1). Nevertheless, uniform Au@Fe_xO_y core–shell composite structures have seldom been studied due to the synthetic challenge and the inactivated properties of the Au core inside the magnetic shell.

Generally, the Fe_xO_y@Au core–shell structure can be achieved either by attaching a uniform Au layer to a Fe_xO_y@Au core-satellite composite or by directly coating a Fe_xO_y core with an Au layer. The application of an Au shell to any material requires reduction of $HAuCl_4$ in an aqueous solution.

A simple but efficient route for the synthesis of spherical Fe_3O_4@Au NPs (Type IA) has been developed by our group recently.[67] Using our method, the resulting Fe_3O_4@Au NPs have a size of $\sim$20 nm and strong magnetization via sodium citrate-coated Fe_3O_4 NPs; sodium citrate is used as the sole reducing agent (as shown in Fig. 2). Cui et al.[68] presented a synthetic method for the core–shell NPs with a typical size of 50 nm in diameter and practical use of the particles in a solid-phase immunoassay. Xu et al.[69] described facile synthesis of Au and Ag-coated Fe_3O_4 NPs with controlled plasmonic and magnetic properties. The plasmonic properties of these core–shell NPs can be fine-tuned by varying the coating thickness and coating material. Wu et al.[70] published a sonochemical method for the synthesis of high-saturation magnetization Fe_3O_4@Au NPs via a 3-step process in the following order:

(a) use a copreparation method to create the Fe_3O_4 core of NPs;
(b) functionalize the Fe_3O_4 NPs with an amine group by means of APTES ([3-aminopropyl]triethoxysilane); and
(c) reduce Au^{3+} ions to form the gold coating using sonolysis.

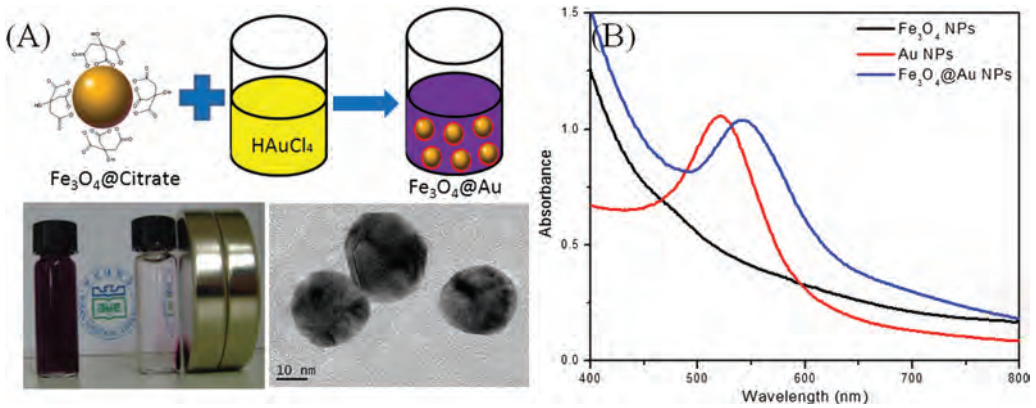

Figure 2. (A) Illustration and a transmission electron microscopy (TEM) image of Fe_3O_4@Au NP preparation. (B) UV-Vis spectra of Fe_3O_4@Au NP colloid solutions. Reprinted with permission from [67], H. Zhou, et al., Ultrasensitive DNA monitoring by Au–Fe_3O_4 nanocomplex. *Sensor Actuat. B-Chem.* 163, 224 (2012). © 2012, Elsevier.

Bao et al.[71] reported the synthesis of γ-Fe_2O_3@Au NPs with varying Au shell thickness by reducing $HAuCl_4$ on the surface of γ-Fe_2O_3 NPs.

Bao et al.[40] reported that the synthesis of multifunctional core-satellite Fe_3O_4@Au NPs (Type IB) occurs via the chemical bonds of 2 separate prepared nanomaterials, not via a chemical deposition process. This synthesis can be used for isolation of a protein, which would still retain strong catalytic activity afterwards. The as-prepared bifunctional NPs combine the merits of both gold and Fe_3O_4 NPs and are formed via chemical bonds. Containing approximately 12% gold by weight, the resulting bifunctional NPs maintain excellent magnetic properties. Umut et al.[72] tested Au@Fe_3O_4 hybrid nanoparticles with the core–shell topology (Type IC). All their particles were linked with oleic acid and oleylamine: 2 organic molecules included as a surfactant during the synthesis process; the surfactants prevent aggregation of particles and increase biocompatibility.

Such core–shell nanostructures could find applications that exploit the electronic, magnetic, catalytic, sensing, and chemical or biological properties of the nanocomposite materials. For utilization of the magnetic properties, the formation of a gold shell with a controllable assembly allows for better stability and tunability for construction of ordered arrays.[3] In a recent study of nanoscale gold, excellent catalytic properties for water-gas shift reactions were found in gold NPs based on an iron oxide core.[73] For the development of applications in biology and medicine, the magnetic NPs and the magnetic field can be used *in vivo* or *in vitro* for either remote positioning or selective filtering of biological materials. In MRI, the presence of the particles at a given site can enhance the contrast of certain types of cells by several orders of magnitude. The possibility of using magnetic NPs to improve the effectiveness of cell manipulations and DNA sequencing could also aid the development of pharmaceuticals, drug delivery systems, and magnetic separation technologies for rapid DNA sequencing. These applications should benefit a great deal from the ability to control the surface and interparticle spatial properties of the magnetic NPs.

Heterodimeric Nanoparticles (Type II)

Heterodimeric Au–Fe_xO_y NPs (denoted as Type II in Fig. 1) are distinct monodispersed NPs that are composed of 1 Au NP and 1 Fe_xO_y NP, bonded interfacially. The bonding is generally achieved via sequential growth of the second component on a preformed NP seed. This approach is similar to the synthesis of core–shell NPs with the difference being that the nucleation and growth are anisotropically centered on 1 specific crystal plane of the seed NP, and not uniformly distributed throughout the seed NP surface. Therefore, the successful synthesis of heterodimer NPs strongly depends on promotion of heterogeneous nucleation while suppressing homogeneous nucleation. This result can be achieved by tuning the seed-to-precursor ratio and controlling the heating profile so that the concentration of the precursor stays below the homogeneous nucleation threshold throughout the synthesis process.[74] In the growth process, the lattice spacing of the 2 components is generally well matched to lower the energy required for epitaxial nucleation of the second component.[75] A lattice mismatch, however, can also be utilized to make heterodimeric NPs via a surface dewetting process of the core–shell structure.[76] Electron transfer at the interface of the 2 components during the nucleation process likely plays a key role in controlling the heterodimer morphology, and this transfer process can be modulated by polarity of the solvent.[77]

Two reaction strategies have been developed for heterodimeric (Type IIA) Fe_3O_4@Au nanocomposites utilizing 50 nm polyethyleneimine-coated magnetite as a seed, designed for diverse practical applications.[78] The polyethylenimine (PEI)-coated Fe_3O_4 NPs were first used as seeds to carry out the synthesis of heterodimeric Fe_3O_4@Au nanocomposites (Figs. 3(A) and (B)). This

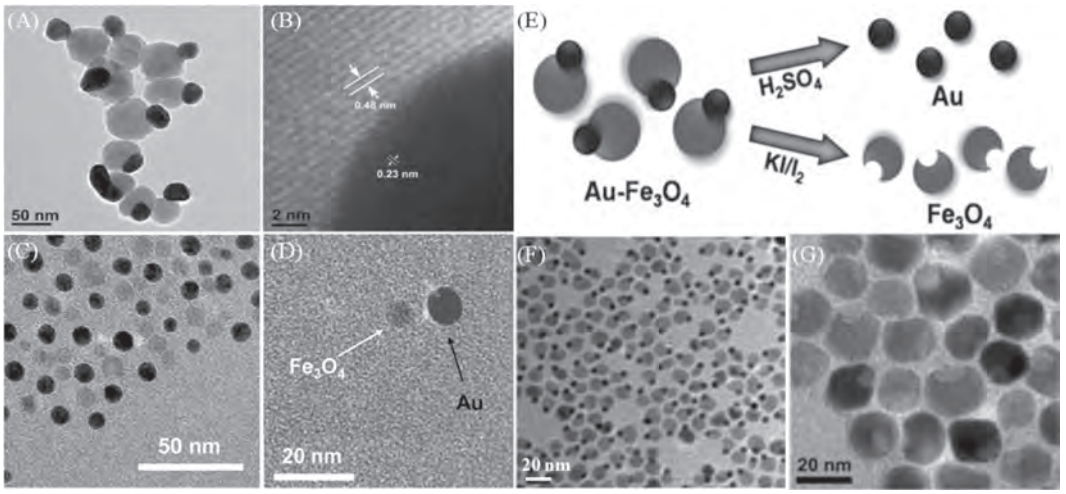

Figure 3. **(A) Transmission electron microscopy (TEM) and (B) HRTEM images of heterodimeric Fe_3O_4@Au nanocomposites; (C) and (D) water-soluble Au-PEG–Fe_3O_4-conjugated nanoparticles (NPs); (E) schematic representation of selected etching of Au–Fe_3O_4 NPs for the preparation of the Au NPs and dented Fe_3O_4 NPs; TEM images of the as-synthesized (F) 6–17 nm Au–Fe_3O_4 NPs obtained using Au as seeds; (G) dented 17 nm Fe_3O_4 NPs obtained by etching Au away from the Au–Fe_3O_4 NPs. Reprinted with permission from [78], L. Lou, et al., Facile methods for synthesis of core–shell structured and heterostructured Fe_3O_4@Au nanocomposites. *Appl. Surf. Sci.* 258, 8521 (2012). © 2012, Elsevier; From [79], M. Wang, et al., Cross-linked heterogeneous nanoparticles as bifunctional probe. *Chem. Mater.* 24, 2423 (2012). © 2012, American Chemistry Society; From [80], Y. Lee, et al., Synthetic tuning of the catalytic properties of Au–Fe_3O_4 Nanoparticles. *Angew. Chem.* 122, 1293 (2010). © 2010, John Wiley & Sons.**

distinct morphology is suitable for diverse applications: the heterodimer structure offers particles with 2 distinct surfaces and functionalities due to different surfactant molecules on the surface of Fe_3O_4 and Au NPs.

The work presented by Wang et al.[79] demonstrated a facile approach to synthesis of multifunctional nanomaterials based on a phase transfer protocol for the cross-linking of NPs via a polyethylene glycol (PEG)-based ligand. Heterogeneous conjugates containing gold and iron oxide NPs (Type IIB) were synthesized and applied as contrast agents to bifunctional scanning confocal microscopy and MRI. Figure 3 (panels C and D) show the transmission electron microscopy (TEM) images of the as-prepared Au-PEG–Fe_3O_4 conjugates. Both binary conjugates with one-to-one correspondence between Au and Fe_3O_4 and ternary structures with 2 Au to 1 Fe_3O_4 or 1 Au to 2 Fe_3O_4 NPs are present in the product (approximately half and half) along with a few individual Au or Fe_3O_4 NPs.

Lee et al.[80] developed a unique synthetic procedure for Au, Fe_3O_4, and Au–Fe_3O_4 NPs. The single-component Au and Fe_3O_4 NPs are produced directly from the Au–Fe_3O_4 NPs using either Au etching or Fe_3O_4 etching, which allows for the direct comparison of NP catalysis of H_2O_2 reduction and shows that the Au–Fe_3O_4 NPs offer enhanced catalysis (as shown in Figs. 3(E)–(G)). By studying the H_2O_2 reduction catalyzed by the individual Au and Fe_3O_4 NPs, researchers can demonstrate experimentally that the enhanced catalysis by Au–Fe_3O_4 arises from the polarization effect at the Au–Fe_3O_4 interface, where Fe_3O_4 becomes more active.

Multicomponent Hybrid Nanoparticles (Type III)

Self-assembly processes provide an approach to fabricate multicomponent hybrid NPs with integrated multifunctionality. The advantages of such multicomponent structures lie in acquisition of novel properties and implementation of multifunctionality and unique applications.[52] By employing intermolecular forces, it is easy to prepare assembled nanostructures from various individual NPs using a carrier material, as shown in Figure 1 (Type III). Both silica and polymer matrices can be used as a carrier material, as discussed below, resulting in a construct that is generally larger than particles of Type I or Type II. This section focuses on multicomponent hybrid NPs using silica capsules as a carrier material due to its low cytotoxicity and useful porous structure.

Porous silica materials possess unique properties such as large surface area, large pore volume, and low cytotoxicity.[81] Nanoparticles embedded in porous silica have many advantages over metal core NPs and metal core-silica shell nanostructures in terms of providing light paths and a convenient reaction environment.[82] These porous shell-coated functional nanomaterials are useful in many respects, such as catalysis, electronics, and encapsulation of drugs.[83] The porous silica shell does not affect the optical and catalytic properties of Au NPs significantly. On the other hand, it simultaneously acts as a protective layer for magnetic and gold NPs preventing the aggregation and oxidation. With this goal, Chen et al.[84] developed the synthesis of this kind of a novel magnetic-gold bifunctional nanocomposite consisting of

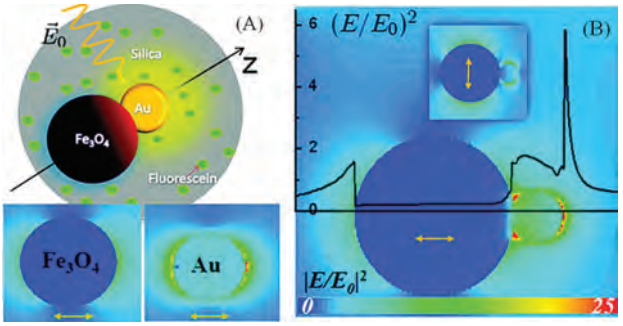

Figure 4. (A) The model used for electromagnetic discrete dipole approximation calculations and the electric field distribution of Fe_3O_4 and Au nanoparticles (NPs; insets), 15 and 5 nm in diameter respectively. (B) The electric field distribution of Au–Fe_3O_4 NPs embedded in a silica medium when the incident electromagnetic wave along the *Z* direction is polarized along the symmetry axis and perpendicular to it (inset). Reprinted with permission from [86], X. F. Zhang, et al., Multifunctional Fe_3O_4–Au/porous silica@fluorescein core/shell nanoparticles with enhanced fluorescence quantum yield. *J. Phys. Chem. C* 114, 18313 (2010). © 2010, American Chemistry Society.

Au–Fe_3O_4 nanocomposite cores and a porous silica shell (Type IIIA).

Inspired by the dual functions of dumbbell-like iron oxide-metal nanoparticles,[80,85] Zhang et al.[86] designed a synthetic procedure for fluorescein-doped nanoporous silica NPs with dumbbell-like Au–Fe_3O_4 cores (denoted as Au–Fe_3O_4/porous silica@F, Type IIIB). By incorporating the fluorescein molecules inside nanoporous shells, Au–Fe_3O_4/porous silica@F NPs exhibit enhanced fluorescence quantum yields compared to Fe_3O_4/porous silica@F NPs (as shown in Fig. 4). Compared to conventional fluorescence-enhanced systems such as Au NPs and Au flat surfaces, Au–Fe_3O_4/porous silica@F nanoparticles (with both magnetic and plasmonic properties) provide advantages for a wide range of practical applications including multimodal imaging and magnetically targeted drug delivery.

The above examples show that multicomponent hybrid NPs using silica as a carrier material can be synthesized in many flavors. Clear advantages of this versatile approach are, for example, the high payload of magnetic NPs and Au NPs that can be integrated, the tunability of the ratio between the NPs, and fine control over the distance between magnetic NPs and Au NPs. Furthermore, the surface plasmon resonance (SPR) of the Au NPs can be easily varied by integrating (a combination of) different Au NPs, allowing for multiplexing of *barcoding*.[87] The surface chemistry of silica particles is well developed, facilitating the biofunctionalization of this carrier. A distinct and inherent feature of the combination of a carrier material with nanocrystals is the relatively large size (> 50 nm). This feature likely poses a limitation for hitting extravascular targets (in drug delivery), but enhances the suitability of this construct for targeting receptors on the endothelial cells of blood vessels. In addition, renal clearance of these larger particles does not occur, which probably increases their blood circulation half-life. This property may be considered an advantage in some cases, but will limit clinical applications.

Nonspherical Core–Shell Architecture of Magnetic and Gold Nanomaterials (Type IV)

Controlled synthesis of metallic NPs with uniform geometry has been a fascinating research area for decades because of the broad use of noble metal NPs in catalysis, photonics, electronics, plasmonics, optical sensing, biological labeling, imaging, and photothermal therapy.[88,89] The properties of novel metallic nanocrystals are strongly influenced by their size, shape, and surface structure.[15,90] In the past several years, a lot of attention has been focused on the fabrication of nonspherical metallic NPs.[91,92] The formation of nonspherical particles is driven by local anomalies and kinetic differences in the growth rate in the different parts of NPs. In general, unlike atoms and molecules, nonspherical NPs lack the ability to grow along specific directions, and therefore, they are thermodynamically unstable and transform into spherical particles with time.[93] Therefore, the synthesis conditions need to be delicately optimized to control the epitaxial growth mechanism allowing for formation of anisotropic NPs. Upon sufficient control over the NP geometry, nonspherical nanoscale entities can be attractive materials because their chemical, structural, biological, and optical properties are expected to be quite different from those of ideal spherical particles. The high degree of sophistication and synthetic control achieved in the case of standard spherical NPs, exemplified by the constantly growing variety of core–shell nanostructures, is also required for nonspherical NPs. Au-coated magnetic NPs (MNP@Au NPs) have received considerable attention over the past decades because of their bifunctionality that allows for combining magnetic and optical properties for a variety of applications.[55]

The final category of particles that will be discussed here is defined as nonspherical core–shell MFMP NPs, schematically shown as Type IV in Figure 1. In any case, the formation of nonspherical particles is driven by kinetic factors, provisionally created in the reaction system. Significant progress has been achieved in controlling the number and length of branches. For example, gold monopod, bipod, tripod, tetrapod, and urchinlike particles have been successfully synthesized using different epitaxial growth approaches. Although the mechanism underlying the growth of nonspherical particles is gradually clarified,[88] fine-tuning the structure and size of nonspherical core–shell particles is still a challenge.

Levin et al.[94] reported the combination of resonant optical and magnetic properties in a single nanostructure, accomplished by means of the growth of an Au shell layer around a magnetic iron oxide core NPs. They show that wüstite (Fe_xO) nanocrystals,[95] which can also form

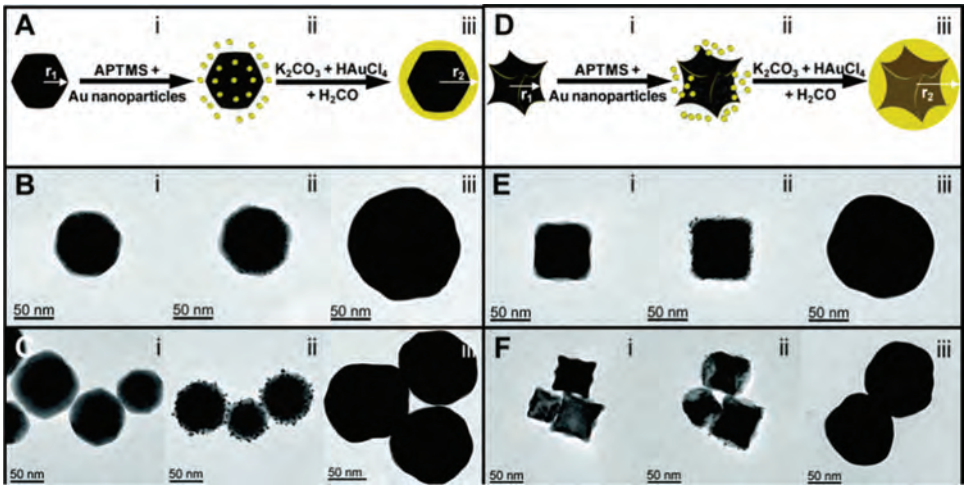

Figure 5. **A schematic of Au-coated iron oxide synthesis for (A) faceted and (D) tetracubic (i) core, (ii) Au-decorated precursor, and (iii) Au-coated iron oxide nanoparticles (NPs); transmission electron microscopy (TEM) images representing various stages of synthesis for (B), (C) faceted and (E), (F) tetracubic (i) core (with average $r_1 = 31.5 \pm 9.7$ and 28.5 ± 7.3 nm), (ii) Au-decorated precursor of NPs, and (iii) Au-coated iron oxide NPs. Reprinted with permission from [94], C. S. Levin, et al., Magnetic-plasmonic core–shell nanoparticles. *ACS Nano* 3, 1379 (2009). © 2009, American Chemistry Society.**

compounds of higher oxidation states, can be used as a magnetic core material and a precursor for continuous gold shell layer growth. The wüstite nanocrystals can be grown in a variety of shapes and sizes; however, the subsequent addition of an Au layer on the nanocrystal surface modifies the overall nanoparticle shape, resulting in spherical or near-spherical morphology with a nonspherical core (Fig. 5).

Nonspherical NPs with complex angled shapes and non-Platonic geometry attract researchers by unique shape dependence of different properties including optical, magnetic, catalytic, and biological. Their reliable preparation—especially in cases when the core–shell morphology determines the function—represents considerable synthetic challenges. Recently, our group[96] reported a synthetic route for creation of magnetoplasmonic supraparticles (SPs) of a spiky shape, tunable diameters (ca. 95–185 nm), plasmonic range 600–700 nm, and strong magnetization. Illustration of the synthetic chemistry for these spiky Fe_3O_4@Au NPs is presented in Figure 6. Citrate-coated Fe_3O_4 NPs were initially prepared as the central cores and subsequently coated with Au layers. The spiky morphology was obtained via the synthesis and attachment of additional Au NPs through seed-mediated reduction of $HAuCl_4$ with hydroquinone. Owing to their bifunctional nature and a combination of magnetic and optical properties and unique geometry, these spiky Fe_3O_4@Au nanostructures can be potentially used in various optoelectronic devices and in certain biomedical applications.

A novel dendritic nanostructure of Fe_3O_4@Au NPs has been fabricated recently using a facile method.[97] The dendritic Fe_3O_4@Au NPs show a mean particle size of 35 nm, intense near-infrared (NIR) absorbance at 754 nm, and strong superparamagnetism, implying the potential applications in the fields of the optical/magnetic-resonance bimodal imaging, photothermal-magnetothermal combined therapy, low temperature catalysis, and magnetic separation. Hui et al.[98] reported a convenient method for synthesis of novel Fe_3O_4@Au@Fe_3O_4 nanoflowers that integrate hybrid components and surface structures. Relative to conventional NPs with the core–shell configuration,

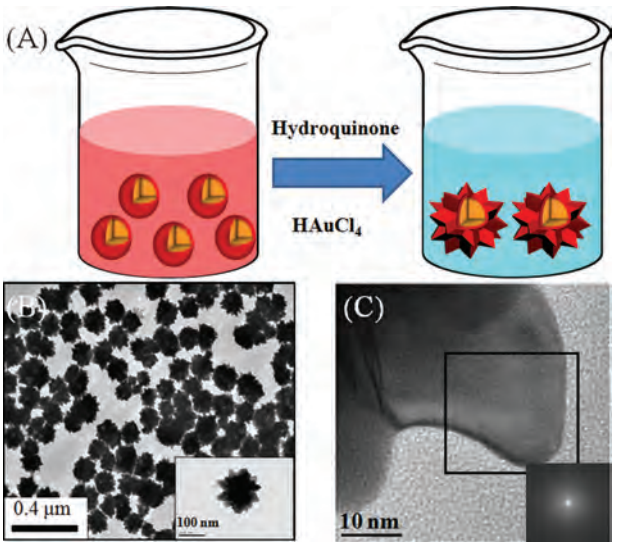

Figure 6. **(A) Illustration of the synthetic chemistry for spiky Fe_3O_4@Au supraparticles (SPs) through seed-mediated reduction of $HAuCl_4$ with hydroquinone. (B) Transmission electron microscopy (TEM) images of spiky SPs; insets show magnified images of the individual SPs. (C) An HR-TEM image and the SAED pattern of 1 branch of the spiky SPs. Reprinted with permission from [96], H. Zhou, et al., Self-assembly mechanism of spiky magnetoplasmonic supraparticles. *Adv. Funct. Mater.* 25, 1439 (2014). © 2014, John Wiley & Sons.**

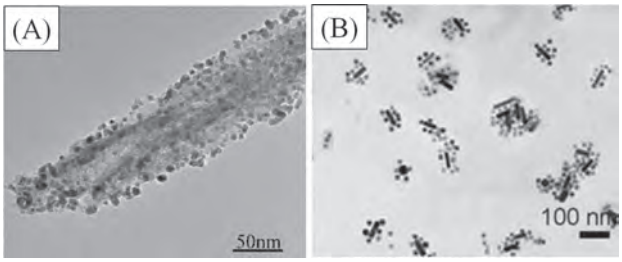

Figure 7. **(A) TEM image of Fe_3O_4–Au hybrid nanorods synthesized by annealing of FeOOH–Au hybrid nanorods under Ar atmosphere; (B) TEM image of Au_{rod}–$(Fe_3O_4)_n$ which is Fe_3O_4 nanoparticles assembled onto the surface of Au_{rod} stabilized by PEG. Reprinted with permission from [99], H. Zhu, et al., Fe_3O_4–Au and Fe_2O_3–Au Hybrid nanorods: Layer-by-layer assembly synthesis and their magnetic and optical properties. *Nanoscale Res. Lett.* 5, 1755 (2010). © 2010, Springer; From [100], C. Wang, et al., Gold nanorod/Fe_3O_4 nanoparticle "nano-pearl-necklaces" for simultaneous targeting, dual-mode imaging, and photothermal ablation of cancer cells. *Angew. Chem.* 121, 2797 (2009). © 2009, John Wiley & Sons.**

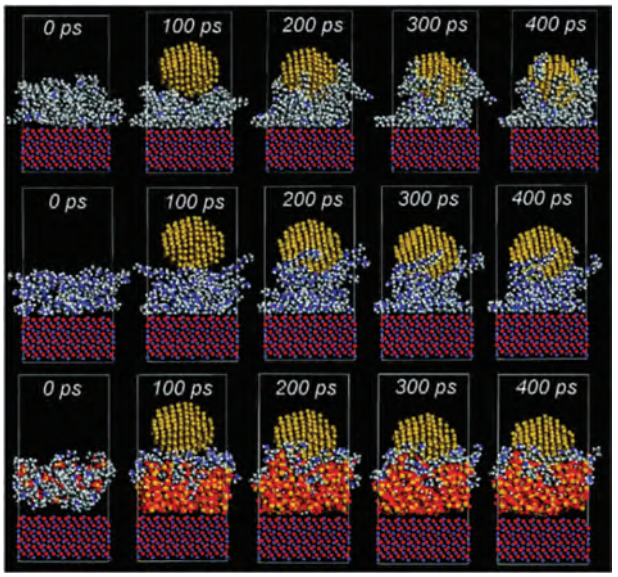

Figure 8. **Snapshots of oleylamine (OM; top), polyethylimine (PEI; middle), and 3-aminopropyltriethylsilane (APTES)-silica coating (bottom) of the surface of Fe_3O_4 (111) and the addition of an Au NP at various time points. Reprinted with permission from [115], J. Yue, et al., Molecular dynamics study on Au/Fe_3O_4 nanocomposites and their surface function toward amino acids. *J. Phys. Chem. B* 115, 11693 (2011). © 2011, American Chemistry Society.**

such nanoflowers not only retain their surface plasmon properties but also allow for a 170% increase in the saturation magnetization and a 23% increase in the conjugation efficiency because of the synergistic cooperation among the hierarchical structures. These novel building blocks could open up novel and exciting vistas in nanomedicine for broad applications such as biosensing, cancer diagnostics and therapeutics, targeted delivery, and high-contrast imaging.

A layer-by-layer technique has been developed for synthesis of FeOOH–Au hybrid nanorods that can be transformed into Fe_2O_3–Au and Fe_3O_4–Au hybrid nanorods via a controllable annealing process.[99] The homogenous deposition of Au nanoparticles onto the surface of FeOOH nanorods can be attributed to the strong electrostatic attraction between metal ions and polyelectrolyte-modified FeOOH nanorods. The annealing atmosphere controls the phase transformation from FeOOH–Au to Fe_3O_4–Au and α-Fe_2O_3–Au. The morphological and structural characteristics of Fe_3O_4–Au hybrid nanorods are shown in Figure 7(A).

Wang et al.[100] demonstrated a novel route for the synthesis of multifunctional *nano-pearl necklaces* based on Fe_3O_4 nanoparticles decorating Au_{rod} that can be used as an MRI and fluorescence imaging agent to target cancer cells. An additional function, i.e., applicability to photothermal therapy, will also be demonstrated. Figure 7(B) illustrates the fabrication of novel nano-pearl necklace multifunctional NPs comprising a single, amine-modified Au_{rod} decorated with multiple "pearls" of Fe_3O_4 nanoparticles carrying COOH groups. Then Au_{rod}–Fe_3O_4 nano-pearl necklaces (abbreviated as Au_{rod}–$(Fe_3O_4)_n$, where $n > 5$) are further stabilized with thiol-modified polyethylene glycol (SH-PEG, $M_W \sim 5000$) and functionalized with herceptin as multifunctional bioprobes for targeting, dual imaging, and photothermal killing of human breast cancer cells (SK-BR-3 cells).

Nanoporous gold fabricated using the dealloying of binary Au alloys has a 3-dimensional network of fine ligaments on the nanoscale, which is a novel unsupported gold catalyst with exceptional catalytic activity for CO oxidation. Kameoka et al.[101] reported a new nanoporous structure: a composite formed by alternately layered Au–Fe_3O_4–Au with layer spacing at approximately 200 nm and with porous structure (the pore size is < 20 nm), as shown in Figures 8(D)–(F). The Au–Fe_3O_4–Au manifested much higher catalytic performance in CO oxidation than a previously reported conventional Au–Fe_2O_3 catalyst. The porous Au and porous Fe_3O_4 were responsible for the high activity and high thermal stability respectively. The porous structure is formed via a self-assembly process using a NaOH aqueous solution for dealloying of Al in a conventionally melting Al–Au–Fe alloy precursor with alternately layered Al_2Au–Al_2Fe–Al_2Au structure.

ENHANCED PLASMONIC AND MAGNETO-OPTICAL PROPERTIES OF MAGNETOPLASMONIC NANOMATERIALS

The term magnetoplasmon was first introduced in the early 70s, motivated at the time by a renewed interest in surface plasmons in metals and degenerate semiconductors.[102, 103] The effect of an external magnetic field on the dielectric function of the electron plasma has attracted much research focused on the magnetic field modification of the

propagation properties of surface plasma waves. Later, in the 80s[104–109] and the 90s[110–114] different groups studied the possible effects of bulk and surface plasmon resonance on the magneto-optical (MO) activity of a number of materials systems.

Nowadays, the phenomena associated with systems where plasmonic and MO properties coexist (the so-called magnetoplasmonic or spin plasmonic systems) have become an active area of investigation, and an increasing number of research groups are exploring this field experimentally and theoretically. Both the effects of a plasmon resonance on the MO activity of nanostructures and the magnetic field effects on their plasmonic properties are attracting much interest in terms of basic and applied research.

Specific Surface Plasmonic Properties

Au-coated Fe_3O_4 NPs are an attractive system[49] that has interesting magnetic and optical properties and important biomedical applications because of negligible cytotoxicity of Au. Due to the generally large lattice mismatch between magnetic and gold nanocrystals, the mechanism of MFMP nanomaterial formation has not been fully explained yet, although many researchers succeeded in combining the 2 materials within 1 nanocrystal (as discussed in the second section earlier).[61] Above all, the role the intermediate layer played in the formation of core–shell structures is not fully understood, and methods to obtain quantitative information on the interaction of surface molecules of gold and iron oxide remain a challenging task. This limitation will reduce the possibilities related to the materials used to synthesize these nanostructures. To move beyond the physical phenomena, a theoretical simulation method will be helpful for prediction of the stability and functionality of nanocomposites, particularly for the synthesis of stable particles for *in vivo* applications and safe removal after use.[41]

To understand the mechanism of formation of MFMP nanomaterials, the molecular dynamics (MD) method is used to simulate the interaction of Au NPs depositing onto the modified Fe_3O_4 (111) surface (Fig. 8).[115] Molecules with various functional groups are being evaluated including oleylamine (OM), oleic acid (OA), polyethylimine (PEI), polymethylacrylic acid (PMAA), 3-aminopropyltriethylsilane (APTES), and tetraethylorthosilicate (TEOS). The surface adsorption of amino acid molecules, cysteine, methionine, and arginine, onto Au/PEI/Fe_3O_4 is simulated to understand the possibility of applications to magnetic separation. Snapshots of the simulation show that the nanoparticle (NP) moves slowly toward the surface of Fe_3O_4 (111), while a surfactant or polymer layer gradually moves toward the Au NP and surrounds it. In contrast, the silica layer can only vibrate rather than surround the Au NP due to its inflexible 3D network structure after polymerization.

Optical properties of core–shell MFMP nanostructures, such as the wavelength of the plasmon resonance, the extinction cross-section, and the ratio of scattering to absorption at the plasmon wavelength are critical parameters in the search for the most suitable particles for envisioned applications. Using Mie theory and the discrete dipole approximation (DDA), a researcher can calculate optical spectra as a function of composition, size, and shape of core–shell nanospheres and nanorods. Brullot et al.[116] reported that in the advantageous NIR, magnetoplasmonic nanospheres produced by available chemical methods lack the desirable tunability of optical characteristics, but magnetoplasmonic nanorods can reach the desired optical properties at chemically attainable dimensions.

Calculated optical properties of core–shell nanospheres with an R_{core} of 5 nm or 15 nm and increasingly thinner gold shells are shown in Figure 9. These spectra indicate the shift of λ_{max} as a result of a simultaneous change of the composition and size of the core–shell nanospheres. As expected, calculations showed that a thinner shell exhibits a greater redshift and shows a lower $Q_{extinction}$ due to a decrease in the amount of gold per particle. The calculated results are consistent with experimentally obtained results for similar systems.[61] From Figure 9(A), it is evident that coating of magnetite particles with an R_{core} of 5 nm with a gold shell does not provide efficient tuning of the plasmon band, nor does it yield high $Q_{extinction}$ throughout the NIR. As shown in Figure 9(B), coating a particle of a size near the superparamagnetic limit with a gold shell reveals 2 types—with a 5-nm and 7.5-nm gold shell—to show plasmon bands in the advantageous NIR region. These results indicate a trend in which magnetoplasmonic nanospheres consisting of a larger core show better tunability in the NIR region. Furthermore, small spherical NPs as calculated here, exhibit negligible $C_{scattering}/C_{absorption}$ at λ_{max} because of the size and wavelength dependence of Rayleigh scattering. This effect diminishes their applicability in scattering applications.

Calculated optical spectra of the $Q_{extinction}$ for 3 sets of nanorods are shown in Figures 9(C)–(E). As one can see in Figure 9(C), an increase in the V_{core}/V_{total} ratio causes a redshift. This phenomenon can be explained in the same way as for the core–shell nanospheres: By increasing the V_{core}/V_{total} ratio, the gold shell surrounding the core becomes thinner, which facilitates the coupling of plasmonic modes across the shell, resulting in a redshift. It can also be seen in the same figure that a decrease in absolute $Q_{extinction}$ is observed for an increasing V_{core}/V_{total} ratio. This effect can be explained by the fact that with the increasing V_{core}/V_{total} ratio, the contribution of gold decreases. Figure 9(D) shows the results of calculations on nanorods with different aspect ratios. Redshifts of the longitudinal dipolar plasmon resonance can be observed with the increasing nanorod aspect ratio, accompanied by an increase in absolute $Q_{extinction}$. This phenomenon is consistent with the earlier explanation: the increasing aspect ratio increases the path length for electron oscillation along the long axis, causing a redshift. Figure 9(E) shows that

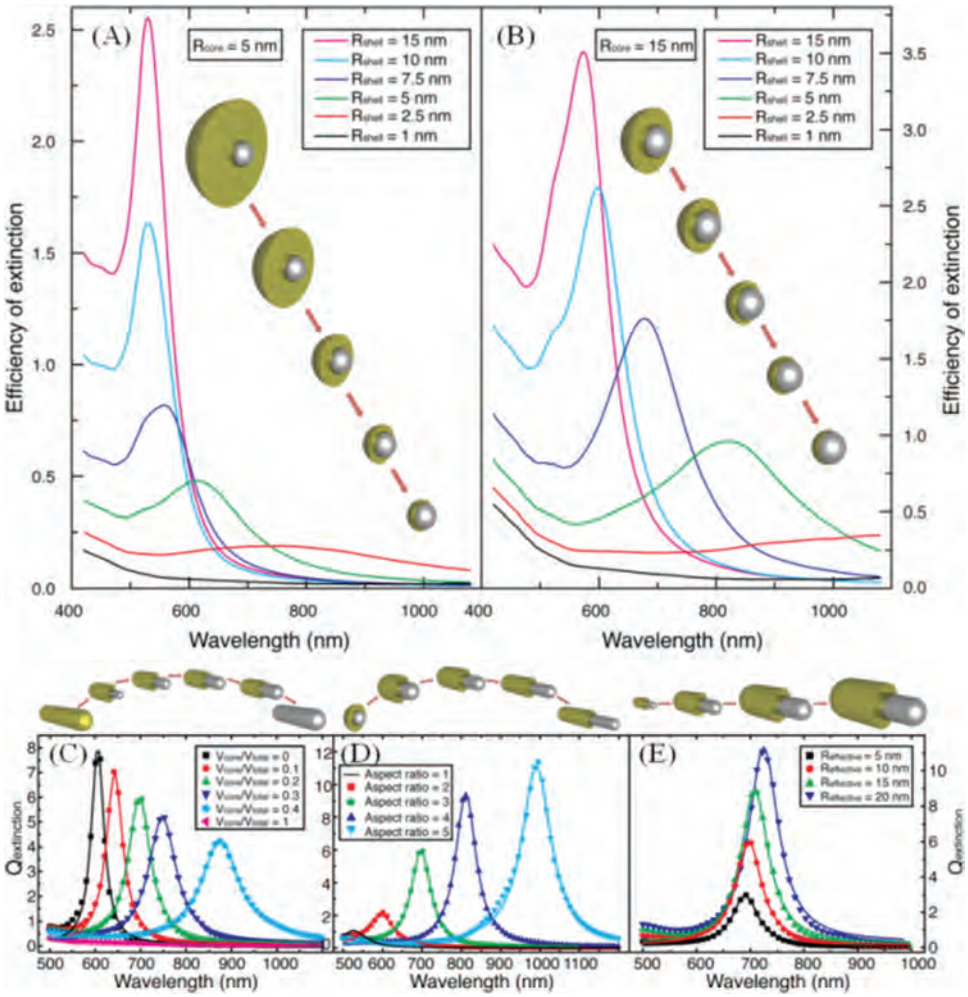

Figure 9. **$Q_{extinction}$ as a function of wavelength for core–shell nanospheres with (A) an R_{core} of 5 nm or (B) an R_{core} of 15 nm and an increasing gold shell thickness (R_{shell}). Calculated optical spectra of the $Q_{extinction}$ for 3 sets of nanorods: (C) Fixed aspect ratio = 3, fixed $R_{effective}$ = 10 nm, and varying V_{core}/V_{total} from 0 to 1; (D) fixed V_{core}/V_{total} = 0.2, fixed $R_{effective}$ = 10 nm, and varying the aspect ratio from 1 to 5; (E) fixed V_{core}/V_{total} = 0.2, fixed aspect ratio = 3, and varying $R_{effective}$ = 5, 10, 15, and 20 nm. Reprinted with permission from [116], W. Brullot, et al., Magnetic-plasmonic nanoparticles for the life sciences: Calculated optical properties of hybrid structures. *Nanomedicine* 8, 559 (2012). © 2012, Elsevier.**

increasing the volume of a nanorod with all other parameters unchanged leads to a modest redshift and an increase of $Q_{extinction}$. As for core–shell nanospheres, the explanation for this phenomenon is that the increase in total size augments the amount of material present in a single nanostructure, enhancing $C_{extinction}$. With this knowledge, it is possible to design and synthesize structures that possess a plasmon band in the advantageous NIR region and other optical properties as needed for a potential application in life sciences.

Magneto-Optical Properties

When a plasmonic material is combined with a magneto-optically active one, the plasmonic and the magneto-optical (MO) properties of the resulting MFMP system become interrelated. In the case of magnetoplasmonic nanomaterials, 2 effects can be attained: (i) there is an increase in the MO activity when surface plasmon polaritons (SPPs) are excited due to the combined action of the intense decrease of the reflectivity and the confinement of the electromagnetic field; (ii) the SPP wave vector can be modified by an external magnetic field due to its dependence on the off-diagonal elements of the dielectric tensor. The former effect can be exploited in magneto-optical surface plasmon resonance (MO-SPR) sensors, whereas the latter phenomenon offers the possibility of developing active plasmonic devices.

More recently, the research efforts shifted to the study of MFMP nanostructures, viz., nanostructures that combine magnetic and plasmonic functions.[117,118] This is because this kind of nanostructures could serve as a building block of a new class of magnetically controllable optical nanodevices for future biotechnological and optoelectronic applications. This new direction in

research has brought forward numerous studies of the effects arising from the mutual interplay between MO activity and light-matter coupling in spatially confined conformations.[119–123] Because plasma oscillations in ferromagnetic materials typically exhibit a stronger damping than in noble metals,[124] a common strategy to overcome this excess damping is to develop hybrid structures consisting of noble metals and ferromagnetic materials, where the noble metal increases the plasmonic response.[125–129]

The theoretical study of the properties of MFMP systems is conducted by means of digital methods mainly. For example, in the work by García-Martín et al.[130] the numerical solution of Maxwell's equations was used to examine a magnetoplasmonic system consisting of an array of cylindrical NPs. It is advantageous, however, to have a simple and straightforward tool that allows for the estimation of the MO properties of complex systems, consisting of magnetic and plasmonic components. In this case, analytical approaches have to be developed. In this respect, the *s*-matrix propagation method was applied by Bonod et al.[131] to treat analytically the structural properties to optimize the surface-plasmon enhancement of the MO effects. Particularly, it was shown that the most effective enhancer of the MO effects is the high-quality surface plasmons for the transverse excitation geometry and may be the overdamped surface plasmons for the polar and longitudinal ones.[131] Makarov et al. put forth an analytical approach based on the Green's function method to assess the MO properties in composite magnetic/nonmagnetic nanoparticles.[132–134] The approach accounts for the local-field effects, and thus allows for estimating correctly the influence of the system shape and dimensions on its MO response. In addition to the localized surface plasmon characteristic of nano-objects, propagating SPPs are of great application relevance[135] in spectroscopy,[136] microscopy,[137] and sensorics,[138–140] to name a few.

CYTOTOXICITY OF MAGNETIC-PLASMONIC NANOMATERIALS *IN VITRO* AND *IN VIVO*

In the past 2 decades, the development and implementation of innovative processes in the field of biomedical engineering were being extensively studied because of the concurrent innovation related to biomedical nanomaterials.[141] Based on the development of composite NPs, MFMP nanomaterials have attracted a broader interest because of their combined advantages of the heteromaterials. Among them, the applications of Fe_xO_y–Au NPs are of practical interest because they have the magnetism of iron oxide that renders them easily manipulable and heated by an external magnetic field. The applications of Fe_xO_y–Au NPs are also interesting because the excellent NIR light sensitivity and strong adsorptive ability of the Au layer can make them useful in biomedical applications.[2] It should be noted that a considerable number of studies have been conducted on the synthesis and the coating process of magnetoplasmonic NPs, but the attention devoted to the biocompatibility for *in vivo* biomedical applications (to ensure safe clinical use of this kind of heteromaterials) is still limited. The basic criteria for their clinical application are safety and good biocompatibility, which are also crucial for industrialization of nanomedicine.[142]

A prerequisite for the implementation of bioapplications of NPs is to obtain NPs with a hydrophilic surface to maintain the colloidal stability under physiological conditions.[143] The most appropriate way to obtain them would be the preparation using aqueous solution-based synthetic approaches. It is a challenge however, to directly obtain monodispersed NPs in aqueous media due to the complexity of controlling the nucleation and growth processes at room temperature, giving rise to particles with low crystallinity, low saturation magnetization, and broad size distribution. Salado et al.[144] reported fabrication of hydrosoluble Fe_3O_4@Au NPs functionalized with biocompatible and fluorescent molecules and their interaction with cell cultures by visualizing them with confocal microscopy. The interaction with cells and the cytotoxicity of the Fe_3O_4@Au, Fe_3O_4@Au-PEG, and Fe_3O_4@Au-glucose NPs were determined upon incubation with the HeLa cell line. These NPs showed no cytotoxicity when evaluated using the MTT assay, and it was demonstrated that the NPs clearly interacted with the cells, showing a higher level of accumulation within the cells for glucose conjugated NPs.

Cytotoxicity of Fe_3O_4–Au NPs and Fe_3O_4–Au NPs loaded with doxorubicin (Dox-Fe_3O_4–Au) combined with an external magnetic field was tested *in vitro* on HepG2 malignant tumor cells by Chao et al.[145] The results showed that cell viability remained above 92% when using Fe_3O_4–Au NPs at a concentration as high as 2.0 mg/mL, suggestive of the biocompatibility of the nanoparticles. The IC_{50} (0.731 μg/mL) of the Dox-Fe_3O_4–Au group was higher than that (0.522 μg/mL) of the Dox group ($P < 0.05$). On the other hand, the Dox-Fe_3O_4–Au group combined with a magnetic field exhibited an obviously increased inhibition rate for the HepG2 cell line and the IC_{50} was lower than that of the Dox group (0.421 μg/mL). These results indicate that Fe_3O_4–Au NPs loaded with doxorubicin combined with a permanent magnetic field are more cytotoxic and could be a potential targeted drug delivery system.

The design of multifunctional NPs for cell imaging and therapeutic applications requires a fundamental understanding of their cellular interactions.[146, 147] The reciprocal response of cells to NPs varies depending on the surface properties of NPs, including composition and morphology, size and shape, and ionic strength.[148] In particular, the surface morphology of NPs is thought to play the most important role in the cellular interactions and systemic distribution of NPs. The ability to manipulate the surface properties of NPs makes improvements in diagnostic sensitivity and therapeutic efficiency possible.[149–151]

Among current nanomaterials, nonspherical core–shell NPs are attractive because of their unique shape-dependent optical and physical properties. As discussed in Section Structure and Synthesis of Magnetoplasmonic Nanoparticles, our group designed 2 shapes of Au-coated iron oxide core–shell NPs, namely, spherical and spiky Fe_3O_4@Au NPs.[67] Recently, we also analyzed the shape effect of the spiky NPs on cytotoxicity and global gene expression in sarcoma 180 cells. Cells treated for 7 days with spiky NP at concentrations up to 50 μg/mL showed $> 90\%$ viability, indicating that these NPs were not toxic. To shed light on the differences in cytotoxicity, the expression of 33315 genes was monitored using microarray analysis of NP-treated cells. The 171 upregulated genes and 181 downregulated genes in spiky NP-treated cells included *Il1b*, *Spp1*, *Il18*, *Rbp4*, and *Il11ra1*: genes mainly involved in cell proliferation, differentiation, and apoptosis.

Li et al. carried out a cytotoxicity assay, a hemolysis test, a micronucleus (MN) assay, and detection of acute toxicity of Fe_3O_4@Au NPs in mice and beagle dogs.[152] The results of the cytotoxicity assay showed that the toxicity grade of this material on mouse fibroblast cell line (L-929) was classified as grade 1, which belongs to no cytotoxicity. Hemolysis rates showed 0.278%, 0.232%, and 0.197%, far less than 5%, after treatment with different concentrations of Fe_3O_4@Au NPs. In the MN assay, there was no significant difference in MN formation rates between the experimental groups and negative control ($P > 0.05$), but there was a significant difference between the experimental groups and the positive control ($P < 0.05$). The median lethal dose of the Fe_3O_4@Au NPs after intraperitoneal administration in mice was 8.39 g/kg, and the 95% confidence interval was 6.58–10.72 g/kg, suggesting that these nanoparticles have a wide safety margin. Acute toxicity testing in beagle dogs also showed no significant difference in body weight between the treatment groups 1, 2, 3, and 4 weeks after liver injection and no behavioral changes. Furthermore, blood parameters, autopsy, and histopathological studies in the experimental group showed no significant differences with the control group. The results indicate that Fe_3O_4@Au NPs appear to be biocompatible and safe nanoparticles that are suitable for further biomedical applications.

The above studies have shown that MFMP NPs appear to be biocompatible and safe NPs according to the evaluation of toxicity *in vivo* and *in vitro*. Given that some of the Food and Drug Administration-approved MRI contrast agents are made of Fe_3O_4, Fe_3O_4@Au composite NPs have a potential to be used as safe optical and thermal agents, allowing for the combination of cancer detection and cancer-specific hyperthermic treatment. These studies laid down the experimental foundation for further clinical research and evaluation of this promising material.

BIOMEDICAL APPLICATIONS OF MAGNETOPLASMONIC NANOMATERIALS

Recently, growing interest has been expressed for the development of MFMP NPs using incorporation of gold nanostructures into superparamagnetic Fe_3O_4 NPs that can combine both plasmonic and magnetic properties in a single NP.[153] Therefore, selected applications of MFMP NPs, which include biosensors, bioseparation, multimodal imaging, and therapeutics, are discussed in this section.

Biosensors

The development of sensitive and cost-effective miniature sensors for detection of biological agents is urgently needed in biomedical and environmental sciences.[154] The sensors feature 2 functional components: a recognition element for selective/specific binding with a target analyte and a transducer component for signaling the binding event. The functionalized NPs also work as biosensors, where the NPs with unique physicochemical properties and their surface functionalized ligands act as recognition and transducer components respectively. Recently, multifunctional magnetoplasmonic nanomaterials have been developed for detection of various biological molecules such as proteins and nucleic acids. In this subsection, we mainly review the recent applications of magnetoplasmonic nanomaterials as sensors to detect biological agents.

DNA-Based Biosensors

A novel detection method for DNA point mutations using quartz crystal microbalance (QCM) based on a DNA ligase reaction and Fe_3O_4@Au core–shell NPs probes has been proposed By Pang et al.[155] The synthesized core–shell NPs were used to implement the isolation of DNA probes and amplification of the detected signal. After the DNA ligase reaction and denaturing at an elevated temperature, a biotin-modified probe reacts with avidin on the electrode surface for the perfect match with a target, causing a change of the crystal frequency, whereas no frequency change would be recorded for a mismatched target. The validity of this approach has been demonstrated with the identification of a single-base mutation at the -28 position of an artificial β-thalassemia gene: the wild-type and mutant sequences were successfully discriminated. A detection limit of 4.6×10^{-10} mol/L of oligonucleotides was achieved. Owing to its ease of operation and high sensitivity, it was expected that the proposed procedure might be useful for both research-based and clinical genomic assays.

Recently, our group reported a simple, sensitive, and inexpensive quantitative approach for DNA detection based on the optical properties of gold NPs and Fe_3O_4@Au NPs.[67] We employed a single-step reaction to synthesize Fe_3O_4@Au NPs, as discussed in Section Spherical Core–Shell and Core-Satellite Nanoparticles (Type I). The resulting Fe_3O_4@Au NPs showed good paramagnetic

properties and were coated with thin layers of gold atoms (~10 nm) having an average diameter of ca. 20 nm. We designed 2 probes to recognize target DNA, where Fe_3O_4@Au NPs were employed to facilitate sample separation using an external magnetic field. The Au–Fe_3O_4@Au complexes were also used to generate a color signal and the uncombined Au NPs produced an optical signal. To achieve high sensitivity, Fe_3O_4@Au NPs were employed for the collection of gold nanoprobes that hybridized with complementary target DNA molecules. The Au–Fe_3O_4@Au nanocomplex remains in the solution at a concentration proportional to the concentration of the target DNA and its optical properties allow it to be easily quantified using UV-Vis absorption spectroscopy, as shown in Figure 10. The limit of detection of this method is as low as 0.1 fM.

Immunosensors

MFMP (Fe_xO_y–Au) NPs are a new type of composite particles, which have a typical core–shell structure with iron oxide as the core and a layer of Au deposited on the core surface as the shell. These NPs have the advantages of convenient binding to biomolecules and easy separation using a magnetic field. The MFMP NPs need only a single step for antibody immobilization and have high binding capacity for antibodies. These advantages permit

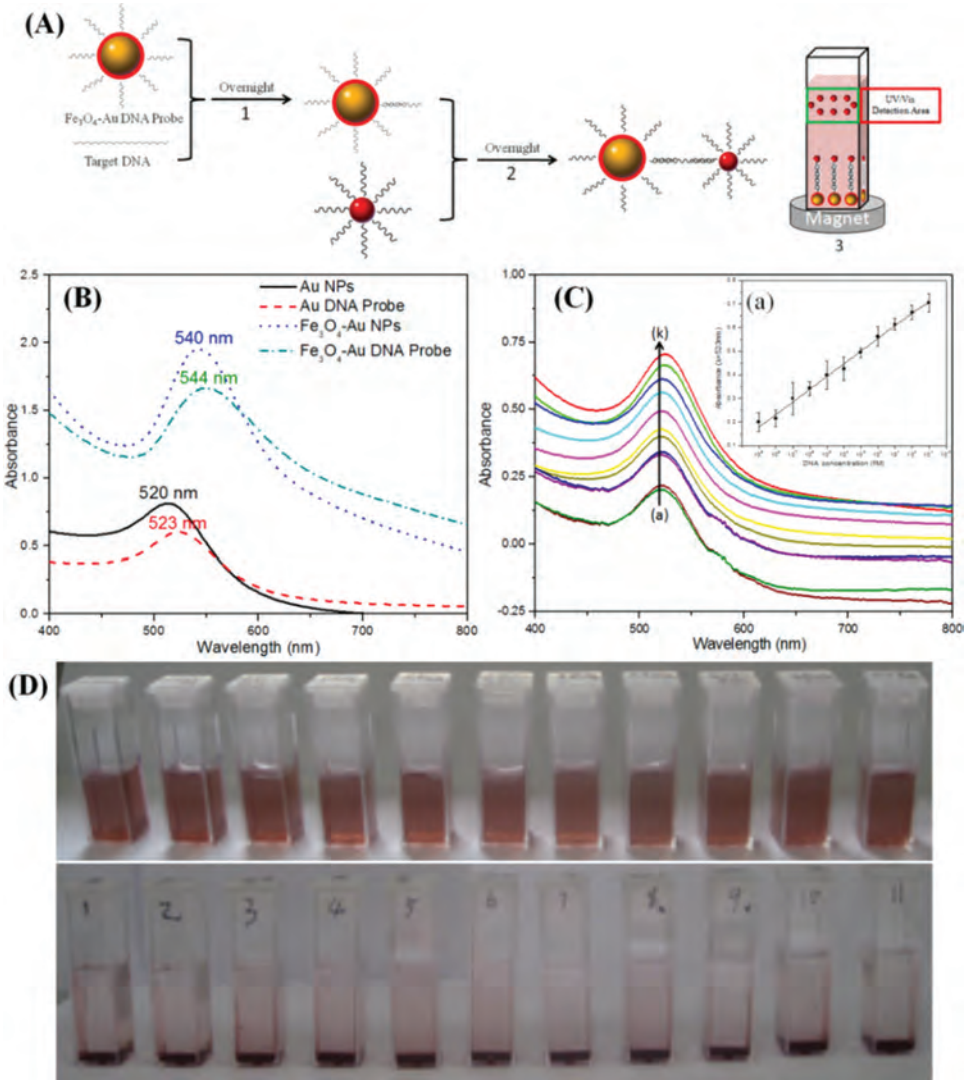

Figure 10. **(A) Illustration of the optical signal of Au nanoparticles (NPs), as used for DNA detection. (B) Comparison of UV-Vis spectra for Fe_3O_4@Au and Au NPs in an aqueous solution; Fe_3O_4@Au–HS-ss-DNA and Au-HS-ss-DNA nanoprobes in a PBS solution. (C) UV-Vis spectra for the different concentrations of target DNA sensor solution: 0.1 μM–0.1 fM → (a)–(k), after we placed the sample on the magnet for 12 h. Insert (a): a calibration curve for colorimetric detection of target DNA spanning the 0.1 fM–1.0 μM concentration range. (D) Photographs display the color change of DNA sensor (different concentrations from 1 μM to 0.1 fM, from left to right) before (top) and after (bottom) we put the sample on the magnet. Reprinted with permission from [67], H. Zhou, et al., Ultrasensitive DNA monitoring by Au–Fe_3O_4 nanocomplex. *Sensor Actuat B-Chem.* 163, 224 (2012). © 2012, Elsevier.**

improved methods of isolating and detecting biomolecules. Using hepatitis B virus (HBV) as a target, Cui et al.[68] have demonstrated that the MFMP NPs can function efficiently as a solid-phase substrate for the detection of HBV antigen in blood. According to the above data, the MFMP NPs provide a great potential for binding an antibody and antigen. Researchers developed an alternative: a new type of immunosensor in the field of immunology promises to be a novel substrate for immunological and affinity-based assays in the near future.

Using MFMP NPs as a carrier, a biotin-avidin amplified enzyme-linked immuno sorbent assay (ELISA) was developed to detect hepatitis B surface antigen (HBsAg).[156] A specific antibody was labeled with biotin and then used to detect the antigen with an antibody adsorbed on magnetoplasmonic NPs by means of a sandwich ELISA assay. The results showed that the biotin-avidin amplified ELISA assay has a higher sensitivity than does the direct ELISA assay. There is a 5-fold difference between HBsAg-positive and -negative serum samples even at a dilution of 1:10000, and the relative standard deviation of the parallel positive serum at a dilution of 1:4000 is 5.98% ($n = 11$). Zhou et al.[157] have successfully synthesized core-satellite Fe_3O_4@Au NPs using a pH-sensitive polyethyleneimine (PEI) linker. The synthesized core-satellite Fe_3O_4@Au NPs were applied to free-PSA detection via a surface-enhanced Raman scattering (SERS) method, which was a convenient way for preconcentrating, purifying, and detecting target proteins in complex biosamples (Fig. 11(A)).

The MFMP Fe_3O_4@Au core–shell NPs can also be prepared for simultaneous fast concentration of bacterial cells by applying an external point magnetic field and for sensitive detection and identification of bacteria using SERS (Fig. 11(B)).[158] A spread of a 10-μL drop of a mixture of 10^5 cfu/mL bacteria and 3 μg/mL Fe_3O_4@Au NPs on a silicon surface can be effectively condensed into a highly compact dot within 5 min by applying an external point magnetic field, resulting in 60 times more concentrated bacteria in the dot area than on the spread area

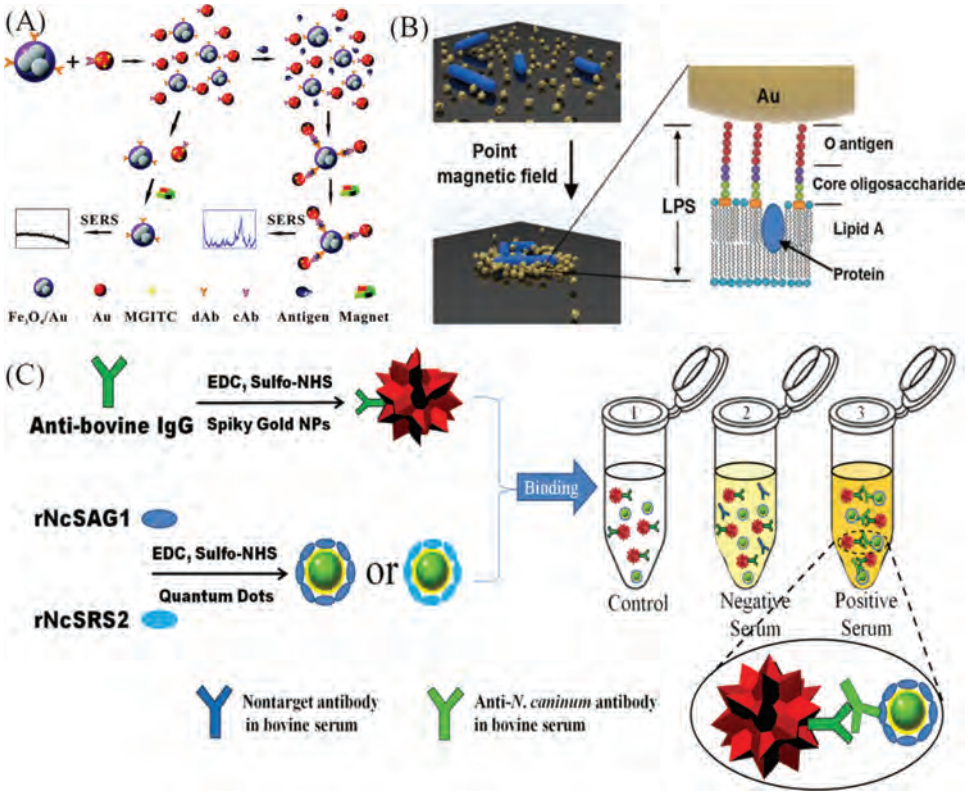

Figure 11. **(A) Schematic illustration of a homogeneous immunoassay using antibody-conjugated Fe_3O_4@Au NPs and Au NPs coupled with a SERS method; (B) Schematics of the condensation process of Au-MNPs and bacteria (left) and the biomolecular characteristics of the bacterial cell wall that can possibly be detected by SERS (right); (C) Schematic representation of the synthesis of antibody-functionalized SNP and CdTe nanocomposite, and the detection mechanism that the biosensor immunoassay employed to capture targets in control, negative serum, and positive serum samples. Reprinted with permission from [157], X. Zhou, et al., Fabrication of cluster/shell Fe_3O_4/Au nanoparticles and application in protein detection via a SERS method. *J. Phys. Chem. C* 114, 19607 (2010). © 2010, American Chemistry Society; From [158], L. Zhang, et al., Multifunctional magnetic-plasmonic nanoparticles for fast concentration and sensitive detection of bacteria using SERS. *Biosens. Bioelectron.* 31, 130 (2012). © 2012, Elsevier; From [160], H. Zhou, et al., Detection of anti-neospora antibodies in bovine serum by using spiky Au–CdTe nanocomplexes. *Sens. Actuator B-Chem.* 178, 192 (2013). © 2013, Elsevier.**

without concentration. Surrounded by dense uniformly packed Fe_3O_4@Au NPs, bacteria can be sensitively and reproducibly detected directly using SERS. The principle component analysis (PCA) showed that 3 Gram-negative bacterial strains can be clearly differentiated. The condensed multifunctional Fe_3O_4@Au NPs dot can be used as a highly sensitive SERS-active substrate; a limit of detection better than 0.1 ppb was obtained in detection of small molecules such as 4-mercaptopyrine.

Wang et al.[159] demonstrated the feasibility of detecting hydrocortisone in cosmetics using a novel CdSe@CdS quantum dot-based competitive fluoroimmunoassay with magnetic core–shell Fe_3O_4@Au NPs as solid carriers. The analyte concentration was quantified by measuring the fluorescence intensity of the unbound hydrocortisone antigen-QDs conjugates. It was observed that with increasing concentrations of hydrocortisone (0.5 to 15000 pg/mL range), the fluorescence intensity was increased. It was shown that the detection limit of hydrocortisone by the test was as low as 0.5 pg/mL.

Very recently, our group[160] reported a rapid, sensitive, and inexpensive qualitative approach to detecting neosporosis based on photoluminescence (PL) enhancement between QDs (CdTe NPs) and a unique form of spiky nanoparticles (SNP). We prepared anti-bovine IgG functionalized SNPs, and a conjugated structure between QDs and a recombinant *N. caninum* protein that was expressed by silkworms. They bound easily when their common complementary target, anti-*Neospora* antibodies (ANABs) in bovine serum, was present. Binding was monitored by the PL enhancement of CdTe NPs in the PL spectrum that resulted from localized surface plasmon resonance (LSPR) of SNPs. Figure 11(C) shows the SNP-CdTe nanocomposite that was used to detect ANABs in bovine serum. The fluorescence intensity of samples from infected and healthy cattle were compared, and significant differences in intensity were found. The SNP-QD sandwich nanocomplexes remained in the solution, and their optical properties allowed for easy quantification using fluorescence spectra. More than 52% emission enhancement on the surface of the SNPs was attained compared with the CdTe NPs and the results were reproducible. Furthermore, the biosensor was suitable for qualitatively analyzing ANABs in blood serum. The ease of operation of this system and its generality offer specific advantages over other immunoassay methods.

Electrochemistry Sensor

With the development of nanoscience and nanotechnology, the combination of various nanoscale materials with enzymes or proteins became possible and may lead to the development of multifunctional nanoassembly systems with simultaneous novel electronic properties. The integration of the technologies will, without a doubt, result in the development of ultrasensitive biosensors relevant to diagnostics, therapy, and controlled drug delivery in the field of health care. Biomolecule-immobilized sensors have found various important applications in many fields such as clinical lab testing, fermentation processes, and pollution monitoring. Within the biosensor research field, the technology based on immobilization of a biomolecule onto an electrode has been stimulating active research because of its reliability, sensitivity, accuracy, ease of use, and a low cost.

A novel dopamine sensor was fabricated by creating 6-ferrocenylhexanethiol ($HS[CH_2]_6Fc$)-functionalized Fe_3O_4@Au NP films on the surface of a carbon paste electrode with the aid of a permanent magnet.[161] $HS(CH_2)_6Fc$, which acted as the redox mediator, was self-assembled into Fe_3O_4@Au NPs via an Au—S bond. The prepared ferrocene-functionalized Fe_3O_4@Au NP composite shuttled electrons between an analyte and the electrode, increased the mediator loading, and prevented the leakage of the mediator during measurements. The electrooxidation of dopamine could be catalyzed by the Fc/Fc^+ couple as a mediator and had a higher electrochemical response due to the unique performance of Fe_3O_4@Au NPs. The nanocomposite-modified electrode exhibited a fast response (3 s) and the linear range was from 2.0×10^{-6} to 9.2×10^{-4} M with a detection limit of 0.64 μM. This immobilization approach effectively improved the stability of the electron transfer mediator and is promising for construction of other sensors and bioelectronic devices.

The magnetic core–shell Fe_3O_4@Au NPs attached to the surface of a magnetic glassy carbon electrode (MGCE) were applied to the immobilization/adsorption of myoglobin (Mb) for fabricating a Mb/Fe_3O_4@Au biofilm.[161] The resultant Fe_3O_4@Au NPs not only have the magnetism of Fe_3O_4 NPs that make them easily manipulated by an external magnetic field but also have the good conductivity and excellent biocompatibility of an Au layer which can maintain the bioactivity and facilitate the direct electrochemistry of Mb in the biofilm (Fig. 12). The modified electrode based on this Mb/Fe_3O_4@Au biofilm displays good electrocatalytic activity to the reduction of H_2O_2 with a linear range from 1.28 to 283 μM. The proposed method simplified the immobilization methodology of proteins and showed the potential application to fabrication of novel biosensors and bioelectronic devices.

Gan et al.[162] have successfully designed a multienzyme labeling Fe_3O_4@Au strategy as part of a signal amplification procedure and demonstrated its use in ultrasensitive, selective, and accurate quantification of α-fetoprotein (AFP) by means of an electrochemical immunoassay. Greatly amplified sensitivity is achieved using bioconjugates where horseradish peroxidase and Ab_2 are linked to Fe_3O_4@Au at a high HRP/Ab_2 ratio for replacement of singly labeled secondary antibodies. The results demonstrated that an immunosensor based on this amplification strategy has a good dynamic range from 0.005 to 10 ng/mL and a good detection limit of 3 pg/mL for AFP.

The as-prepared Fe_3O_4–Au hybrid NPs, which combine the merits of magnetic materials and gold, were

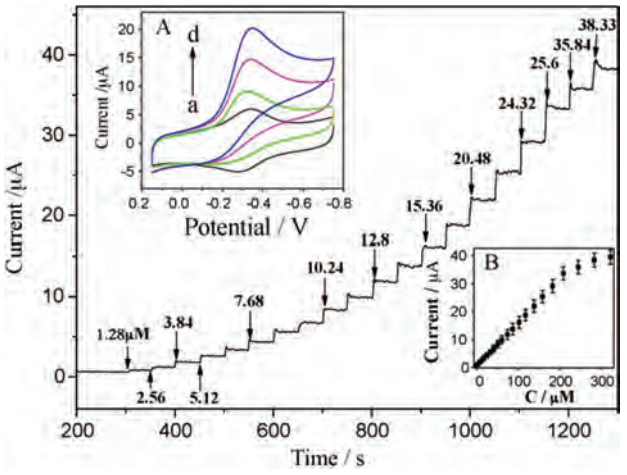

Figure 12. Amperometric responses of the Mb/Fe_3O_4@Au/MGCE at − 0.35 V to successive addition of H_2O_2 in a stirred 0.1 M PBS (pH 6.98); Inset: (Left) Cyclic voltammograms of the Mb/Fe_3O_4@Au/MGCE in 0.1 M pH 6.98 PBS containing 0 (a), 15 (b), 50 (c), and 100 μM (d) H_2O_2 at 100 mV s^{-1}. (Right) Plot of chronoamperometric current versus H_2O_2 concentration. Reprinted with permission from [161], J. D. Qiu, et al., Synthesis and characterization of ferrocene modified Fe_3O_4@Au magnetic nanoparticles and its application. *Biosens. Bioelectron.* 24, 2649 (2009). © 2009, Elsevier.

successfully employed for the first time in the dual-mode detection of carcinoembryonic antigen (CEA) via electrochemical and surface-enhanced Raman scattering (SERS) methods.[163] Both methods make clever use of Fe_3O_4–Au NPs and can accurately verify the presence of antigens. In particular, the electrochemical immunosensor detection has a wide linear range (0.01–10 ng/mL) of response with a good detection limit (10 pg/mL), whereas the SERS method responds to even lower antigen concentrations with a wider detection range.

To sum up, the highlights of the developed electrochemical biosensor using MFMP NPs are: Fe_3O_4@Au as an enzyme-loading carrier can load many enzyme molecules on each Fe_3O_4@Au NP, thus enhancing the sensitivity of the biosensor; using Fe_3O_4@Au as signal enhancers facilitates rapid separation and purification of the signal antibody on an external magnetic field; after each detection, the biosensor can be easily regenerated by applying an external magnetic field. The electrochemical biosensors using magnetoplasmonic NPs have high sensitivity, good reproducibility, stability, and accuracy.

Surface Plasmon Resonance Biosensors

A surface plasmon resonance (SPR) biosensor could be applied to label-free detection of a biomolecule at the metal layer surface, such as Au or Ag.[164] Owing to many advantages such as real-time, label-free and nondestructive detection, the SPR biosensor has been applied to studies of various interaction partners, including proteins,[165] nucleic acids,[166] hormones,[167] cells,[168] and especially antigens.[169] The method for immobilizing biomolecules on the surface of a biosensor chip is crucial for enhancing the sensitivity of an SPR biosensor and for simplifying the immunoassay procedures. The biomolecules have been immobilized on sensor surfaces by means of various techniques, such as sandwich assays, the avidin-biotin system, the labeling of inorganic NPs, and a chemical bond.[170] In most of these methods, a protein is immobilized on the surface of a biosensor using a chemical method. The magnetic NPs have great advantages in the immobilization of proteins on the SPR biosensor.[171, 172] Compared to traditional antibody immobilization on the sensing film, there is no covalent link between the biosensor chip surface and the antibody. With the magnetic property and good biocompatibility, the Fe_3O_4–Au nanocomposites could be an excellent candidate as a carrier for protein immobilization. The conjugates of Fe_3O_4–Au nanocomposites with an antibody can be made on the surface of the biosensor by means of a magnetic pillar easily. With the exceptional optical properties, the Fe_3O_4–Au nanocomposites can play a major role in the enhancement of sensitivity of the biosensor.

Small molecules or analytes present at low concentrations are difficult to detect directly using conventional SPR techniques because only small changes in the refractive index of the medium are typically induced by the binding of these analytes. Recently, Liang et al.[173] presented an amplification technique using core–shell Fe_3O_4@Au NPs for an SPR bioassay. To evaluate this amplification effect, a novel SPR sensor based on a sandwich immunoassay was developed to detect AFP by immobilizing a primary AFP antibody (Ab_1) on the surface of a 3-mercapto-1-propanesulfonate/chitosan-ferrocene/Au NP (MPS/CS-Fc/Au NP) film, employing Fe_3O_4@Au-AFP secondary antibody conjugates (Fe_3O_4@Au–Ab_2) as an amplification reagent. A calibration curve of the Fe_3O_4@Au–Ab_2 conjugate amplification for AFP detection was shown to yield a linear correlation in the range of 1.0–200.0 ng/mL with a detection limit of 0.65 ng/mL. A significant increase in sensitivity was therefore achieved by means of the Fe_3O_4@Au–Ab_2 conjugate as an amplifier. This magnetic separation and amplification strategy have a great potential for the detection of other biomolecules of interest with low interference and high sensitivity by changing the antibody label used in the Fe_3O_4@Au-antibody conjugates.

Wang et al.[174] reported that the core–shell Fe_3O_4@Au NPs modified with 3-mercaptopropionic acid (MPA) were prepared and applied to the SPR biosensor. For their magnetic and exceptional optical properties, the Fe_3O_4@Au NPs were used as the solid support for the goat anti-human IgM, which was immobilized on the surface of the SPR biosensor chip by means of a magnetic pillar. This novel method of immobilization of goat anti-human IgM simplified experimental procedures and facilitated the regeneration of the sensing membrane. As a result, the SPR biosensor exhibits a satisfactory response to human IgM in the concentration range of 0.30–20.00 μg/mL.

Increasing the NP diameter further enhances the sensitivity of the SPR biosensor.

A novel nanocomposite Fe_3O_4–Au NR was prepared and used as a substrate in an SPR biosensor to detect goat IgM.[175] The nanocomposites exhibit both magnetic and exceptional optical properties, which are useful for antibody immobilization and for the sensitivity of detection. Moreover, the Au NR shows 2 plasmon resonance wavelengths defined as transverse mode and longitudinal mode, and the longitudinal plasmon wavelengths are more sensitive to the changes in the dielectric properties of the surroundings. In the optimal conditions, the biosensor based on Fe_3O_4–Au NR nanocomposites exhibits a satisfactory response to goat IgM in the concentration range of 0.15–40.00 μg/mL.

Bioseparation

The biotechnologies today allow proteins to be expressed easily, whereas purification of a low-abundance protein is still a difficult procedure. The development of methods for enrichment and purification of proteins, especially low-abundance proteins, is currently a hot topic. Many target proteins are usually expressed with a tag for affinity separation, and histidine-tagged (His-Tag) fusion proteins are preferably considered for protein preparation. The custom-made products can be conveniently purified using metal chelate affinity chromatography (MCAC) based on the formation and disassociation of the coordination bonds between the 6 consecutive histidine residues ($6 \times$ His) and Ni^{2+}-nitrilotriacetate complex (NTA–Ni^{2+}) under certain conditions.[176–178] The MCAC method is universal: simple in the chemical structure of coordination group and suitable for mild separation conditions; nevertheless, it also has shortcomings such as its tedious operation, low protein binding capacity, and lower efficiency for low-abundance proteins. Magnetic NPs exhibit unique superiority in separation and analysis because of their highly specific surface area, good solubility, and magnetic manipulability. With the development of magnetic NP-based bioseparation and analytical techniques,[24, 41] magnetic NPs have been used successfully to enrich and separate histidine-tagged proteins. The protein-binding efficiency for MCAC with magnetic NPs is much higher than that for micrometer scale packing, with a remarkable decrease in nonspecific adsorption of proteins.[179] Magnetic NPs, however, are prone to aggregation and are surface unstable, and even able to lose magnetism when used in complicated systems; these problems limit their applications. Therefore, it is worth exploiting higher enrichment and separation efficiency and the better detection limit of magnetic NPs used in bioseparation.

Gold NPs have been widely applied to biosensing and immunoassays[180–182] because they have good biocompatibility, chemical stability, and special optical properties and are easy to biofunctionalize. Au NPs can be readily functionalized with thiol groups, for example, using MPA. The Au NPs modified with MPA have been widely used to bind to proteins.[183] Nonetheless, the Au NPs also have a shortcoming. When Au NPs are used in the separation of proteins from a sample solution, multiple rounds of centrifugation are usually required, which is tedious and time consuming. Therefore, MFMP nanomaterials are becoming more and more popular for their integration with magnetomanipulability, stability, and biocompatibility. The MFMP nanomaterials facilitate applications of both gold and magnetic NPs in biology.[40, 71, 77, 184–186] Some MFMP nanomaterials have been used successfully to separate proteins. Bao et al.[71] synthesized Fe_2O_3@Au core–shell NPs and used them for antigen separation and for an immunoassay coupled with surface-enhanced Raman scattering (SERS). Park et al.[185] prepared Fe_3O_4@Au NPs using thermal processing, with the particle size and the shell thickness being controllable, and used the resulting NPs for immunoseparation with SERS detection. Bao et al.[40] fabricated Au–Fe_3O_4 NPs by means of chemical bonding, which were successfully used for protein separation. Xie et al.[187] prepared biofunctionalized magnetic Fe_3O_4@Au–NTA–Ni^{2+} NPs by modifying Fe_3O_4@Au with MPA followed by conjugating with NTA and chelating to Ni^{2+}. Furthermore, maltose-binding protein (MBP) was enriched and separated directly from the mixture of lysed cells with these NPs. Magnetic Fe_3O_4@Au–NTA–Ni^{2+} NPs have been successfully assembled using MPA to modify Fe_3O_4@Au followed by conjugation of NTA and chelating of Ni^{2+}, resulting in biofunctionalized magnetic Fe_3O_4@Au–NTA–Ni^{2+} NPs with strong affinity for His-Tag fusion proteins. These magnetic NPs can efficiently capture, enrich, and purify the MBP directly from the cell lysate.

Liu et al.[2] tested applicability of Fe_3O_4@Au core–shell NPs as a vehicle for biomedical applications such as cell separation. Streptavidin-fluorescein isothiocyanate (STA-FITC) was conjugated to the surface of the Fe_3O_4@Au NPs using a carbodiimide activation protocol (Fig. 13). These NPs were further tested for their ability to bind $CD4^+$ T lymphocytes, which were bound to biotin-labeled anti-CD4 mAbs and isolated from the spleen of C57BL/6 mice. The Fe_3O_4@Au NPs successfully pulled down $CD4^+$ T lymphocytes from the whole splenocytes with high specificity. Therefore, these NPs provide an efficient tool for the cell separation process and further present the dramatic potential to be applied to other areas of biomedicine including diagnosis, monitoring, and treatment of human diseases.

The bioconjugation of Fe_3O_4@Au NPs makes them into carriers of various biomolecules such as DNA, antibodies, and enzymes, which therefore can be used as biorelated functional materials in bioanalytical chemistry, such as affinity extraction and biosensors.[188] The positively charged protein (e.g., antibody or enzyme) can be immobilized on the surface of Fe_3O_4@Au NPs via physical adsorption,[189] but the stability of the adsorbed

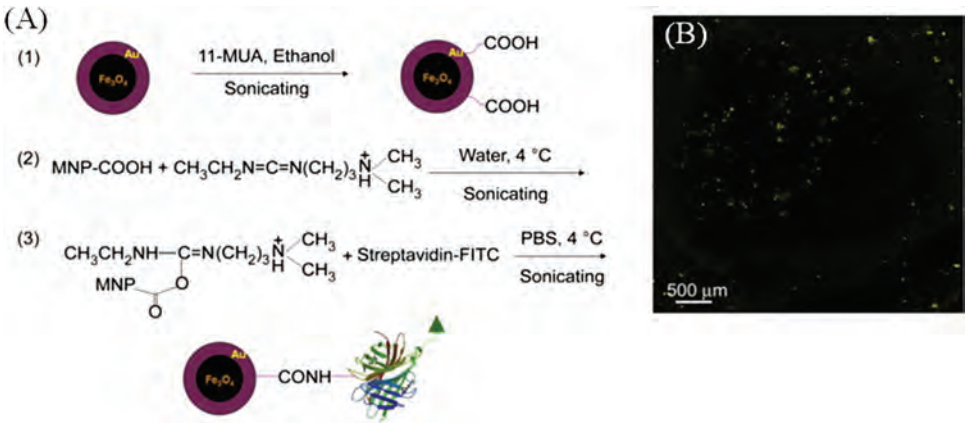

Figure 13. **(A) A flow chart of the synthesis of a Fe_3O_4–Au-straptavidin-FITC nanosystem (Fe_3O_4–Au-STA-FITC). (B) A fluorescent image of streptavidin-FITC-linked Fe_3O_4–Au core–shell nanocrystals. Reprinted with permission from [2], H. L. Liu, et al., Synthesis of streptavidin-FITC-conjugated core–shell Fe_3O_4–Au nanocrystals and their application for the purification of CD4+ lymphocytes. *Biomaterials* 29, 4003 (2008). © 2008, Elsevier.**

protein may be a challenge when used in complex biological samples. This problem can be solved by covalently immobilizing the antibody on Fe_3O_4@Au NPs coated with a protein-coupling agent,[188] but accessibility of the antigen to the binding sites may be sterically hindered because the antibody is randomly immobilized and the length of the intermediate linker is relatively small. In the work of Zhang's group, half-IgG of antiepitestosterone (17α-hydroxy-4-androsten-3-one, abbreviated as *ET*) monoclonal antibodies were immobilized on Fe_3O_4@Au NPs through Au—S bonds and successfully applied to pseudohomogeneous immunoextraction,[190] but the preparation of half-IgG from anti-ET mAbs was complicated and time consuming. Therefore, Zhang's group[191] developed an efficient, economic, and simple new method for nanoparticle bioconjugation recently. In their work, an anti-CD3 monoclonal antibody is bioconjugated to the surface of Fe_3O_4@Au NPs in specific orientation, through affinity binding between the Fc portion of the antibody and protein A that was covalently immobilized on the NPs. The oriented immobilization method was performed to compare its efficiency of cell separation with the nonoriented one, in which the antibody was directly immobilized onto the carboxylated NPs surface. Results showed that the oriented bioconjugated Fe_3O_4@Au NPs successfully pull down $CD3^+$ T cells from the population of whole splenocytes, with high efficiency of up to 98.4%, showing a more effective cell capture nanostructure than that obtained with the nonoriented strategy. The novel strategy for the synthesis and oriented bioconjugation of Fe_3O_4@Au NPs offers an efficient tool for cell separation, and may be applied to various fields of bioanalytical chemistry for *in vitro* diagnosis, affinity extraction, and biosensing.

Multimodal Imaging

Noninvasive imaging of cancer with various modalities to examine a tumor's anatomical structure as well as its metabolism and biochemistry is crucial for early detection of cancer and for early and accurate localization.[192, 193] Existing clinical imaging modalities include computed tomography (CT), magnetic resonance imaging (MRI), positron emission tomography (PET), optical fluorescence, and ultrasound imaging.[194] Each of them possesses characteristic strengths and weaknesses, but none of them is capable of providing complete structural and functional information independently from or superior to all other methods.[195, 196] Thus, it is worthwhile to integrate the strengths of individual modalities to acquire comprehensive information and improve early and accurate detection of tumors. On the one hand, detection with several imaging modalities needs injection of various contrast agents, which is time consuming and inconvenient for patients. In addition, different contrast agents may interfere with one another. The emergence of multimodal contrast agents that are capable of generating contrast in different ways by means of several components will solve these problems.[197–199] They need to be injected only once to complete various imaging modalities. Therefore, multimodal contrast agents can avoid or reduce the mutual interference arising in a mixture of different contrast agents.

Recently, various types of hybrid NPs have been used for multimodal imaging.[200–202] Hybrid NPs, incorporating several components into a single nanostructure system, integrate the strengths of individual components. The hybrid NPs are usually constructed by combining the components of various NPs or by modifying the single-component NPs with some other materials, which is an ideal multimodal contrast agent. Two or more imaging components are encapsulated into a silicon nanoshell, lipid, or some other organic compound.[203–206] Fluorescent dyes or some other molecules used for imaging are modified on the surface of nanoparticles.[207, 208] Two or more kinds of NPs are connected via covalent or noncovalent linkage.[5, 100] Multimodal contrast agents that are formed by

encapsulating multiple NPs together have short circulation time in the blood stream because of their large particle diameters.[209] Moreover, the hybrid NPs constructed using noncovalent linkage are not stable enough.

The MFMP nanomaterials (Fe_xO_y–Au NPs) are hybrid NPs with the gold shell directly deposited onto the iron oxide core. Compared to the majority of the existing multimodal contrast agents, a hybrid NP has stable structure, a controlled particle size, and smooth surface. In addition, it has complementary advantages for various biomedical applications because of the functioning of both the Fe_3O_4 core and gold shell. Fe_3O_4 NPs have been used for various biomedical applications, such as MRI, magnetic separation, and microwave-induced thermoacoustic imaging because of their strong absorption of microwaves.[33, 210] Au NPs have been extensively used in biological applications due to their biocompatibility and absorption properties, which make them good contrast agents for CT and photoacoustic imaging. Their rich history of surface chemistry can also be used for subsequent treatment with some useful chemical or biological molecules. Consequently, magnetoplasmonic nanomaterials have potential uses as a multimodal contrast agent for MRI, CT, microwave-induced thermoacoustic or photoacoustic imaging, and magnetomotive photoacoustic imaging.[211, 212] When conjugated with a fluorescent dye, they can also be used for fluorescence imaging, which has much higher sensitivity than do the above-mentioned imaging modalities. With the magnetoplasmonic nanomaterials, physicians can identify a specific location of a tumor in the body before a surgical procedure, by means of MRI, microwave-induced thermoacoustic imaging or photoacoustic imaging, and then use fluorescence imaging to find and remove all parts of the tumor during the operation.

Multimodal imaging based on complementary detection principles has a great potential for improving the accuracy of tumor diagnosis. Fe_3O_4@Au NPs can be used as an effective multimodal contrast agent because they combine the advantageous and complementary features of the Fe_3O_4 core and a gold shell. Recently, Zhou et al.[213] developed a novel Fe_3O_4@Au NP-based probe for targeting and multimodal imaging of cancer cells. The potential use of the prepared Fe_3O_4@Au NPs as a multimodal contrast probe for MRI, microwave-induced thermoacoustic imaging and photoacoustic imaging was then evaluated. When conjugated with a cancer cell-targeting molecular and fluorescent dye, the Fe_3O_4@Au NPs can be internalized by the corresponding cancer cells selectively, and sensitive fluorescence imaging is implemented at the same time. The biomodified Fe_3O_4@Au NPs incorporating multiple functionalities into a single nanostructured system can be used for effective targeting and simultaneous multimodal imaging of cancer cells.

Cai et al.[214] reported a facile approach for fabrication of Fe_3O_4@Au nanocomposite particles (NCPs) as a dual-mode contrast agent for both MRI and CT imaging applications. The resulting Fe_3O_4@Au NCPs are colloidally stable and hemo- and biocompatible in the given concentration range (0–100 μg/mL). The relatively high r^2 relaxivity (71.55 $mM^{-1} \cdot s^{-1}$) and enhanced X-ray attenuation properties—compared to either uncoated Fe_3O_4 NPs or dendrimer-entrapped gold NPs (Au DENPs)—afford the novel Fe_3O_4@Au NCPs a capacity not only for dual-mode CT and MR imaging of cells *in vitro* but also for MR imaging of liver and CT imaging of subcutaneous tissues *in vivo*. With the facile integration of both Fe_3O_4 NPs and Au DENPs within 1 particle system via the layer-by-layer assembly technique and dendrimer chemistry, the resulting Fe_3O_4@Au NCPs are expected to be further modified with multifunctionality for multimode imaging of various biological systems.

Contrary to the routine chemical processes for preparing Fe_3O_4–Au hybrid NPs, Narayanan et al.[215] reported an environmentally friendly (green) method involving a well-known polyphenol from grapes, viz., grape seed proanthocyanidin (GSP), to simultaneously aid reduction and stabilization of the nanohybrids at room temperature during a completely aqueous synthesis route. MRI and magnetization studies revealed that the Fe_3O_4 component of the hybrid provides superparamagnetism, with dark T_2 contrast and high relaxivity (124.2 ± 3.02 $mM^{-1} \cdot s^{-1}$). PCT imaging demonstrated good X-ray contrast, which can be attributed to the presence of the nanogold component in the hybrid. Considering the potential application

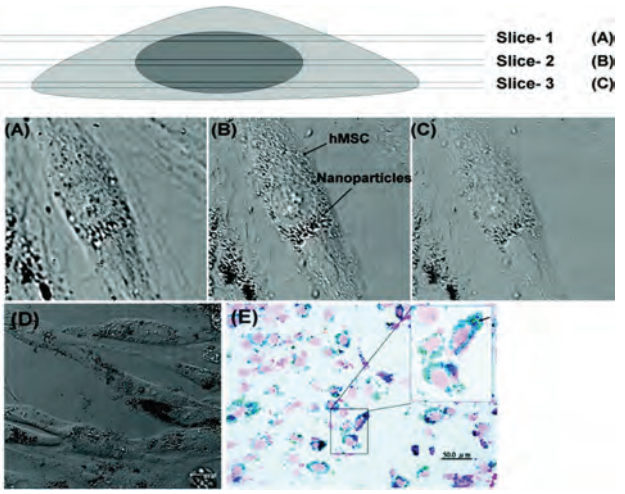

Figure 14. DIC images of human mesenchymal stem cells (hMSCs) taken under a confocal microscope. (A)–(C) Serial optical sections of hMSCs showing hybrid nanoparticles distributed in the cytosol after uptake. (D) A low-magnification DIC image of hMSCs showing nanoparticle uptake, and (E) Prussian blue staining of hMSCs showing the uptake of hybrid nanoparticles as a blue stain. The arrowhead indicates magnetite nanoparticles stained with Prussian blue. Reprinted with permission from [215], S. Narayanan, et al., Biocompatible magnetite/gold nanohybrid contrast agents via green chemistry for MRI and CT bioimaging. *ACS Appl. Mater. Interfaces* 4, 251 (2011). © 2011, American Chemistry Society.

of this bimodal nanoconstruct for stem cell tracking and imaging, the compatibility studies on human mesenchymal stem cells (hMSCs) were carried out, wherein the authors assessed cell viability, apoptosis, and intracellular reactive oxygen species (ROS) generation due to the particle-cell interaction. The material shows good biocompatibility even at high concentrations (500 μg/mL) and incubation up to 48 h, with no apoptotic signals or ROS generation. Cellular uptake of the nanomaterials was visualized using confocal microscopy and Prussian blue staining (Fig. 14).

Therapeutics

As reported during the past decade, plasmonic Au NPs and superparamagnetic iron oxide NPs are promising therapeutic agents.[216–225] If clinical trials are successful, these NPs may be used as targeted therapeutic agents in photothermal therapy. Au NPs of different sizes and shapes with optical properties tunable in the NIR region are useful for cancer imaging as a result of their high transmission rate through biological tissues.[226–228] On the other hand, iron oxide NPs have been used as contrast agents in MRI and biological separation.[229–232] In addition to its biocompatibility, negligible toxicity, and the ability to generate high temperatures at a desired site, the use in the early detection and therapeutic challenges of cancer perhaps is the most promising feature of nanotechnology therapeutics based on plasmonic gold.[12, 233, 234] Similarly, MNPs can also mediate localized hyperthermia effects in the presence of a strong magnetic field.[6, 235–237] As a result, the integration of magnetic and plasmonic functions into a single platform such as a magnetic core with a plasmonic shell would be helpful for cancer nanomedicine. Plasmonic gold coating on magnetic NPs is useful for stabilizing high-magnetic-moment NPs in corrosive biological conditions. It will also allow for easy bioconjugation through the well-developed chemistry of Au—S.[55, 94, 238]

In recent years, many research efforts were focused on developing novel gold nanostructures to achieve surface plasma resonance in the NIR region. Halas and coworkers developed 10-nm-thick gold nanoshells coating 110 nm diameter silica cores with a NIR absorption peak. Those authors demonstrated the use of these NPs in photothermal ablation of cancer cells and cancer tissue.[239] Wang et al. prepared Fe_3O_4@polymer@Au shell–core–shell nanostructures using NH_2OH reduction and seed-induced growth methods and found that the composites

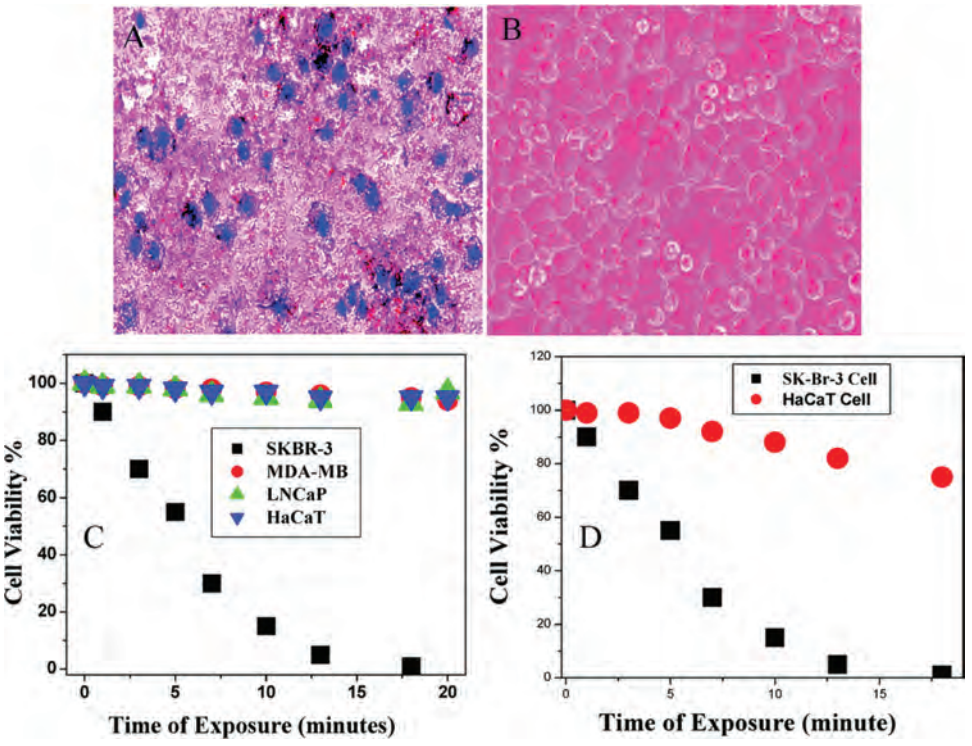

Figure 15. **(A) Bright-field inverted microscopy images of aptamer-conjugated magnetic/plasmonic nanoparticles attached to SK-BR-3 breast cancer cells after irradiation with 670 nm light at 2.5 W/cm^2 for 7 min followed by staining with trypan blue. (B) Bright-field inverted microscopy images of SK-BR-3 cells alone after irradiation with 670 nm light at 2.5 W/cm^2 for 10 min followed by staining with trypan blue. (C) A plot showing cell viability when S-6 aptamer-conjugated magnetic/plasmonic nanoparticles attached to SK-BR-3, MDA-MB, and HaCaT cells were activated using 670 nm light at 2.5 W/cm^2 for 20 min. (D) A plot showing cell viability when S-6 aptamer-conjugated magnetic/plasmonic nanoparticles attached to SK-BR-3 and HaCaT cell mixtures (1:0.01) were activated with 670 nm light at 2.5 W/cm^2 for 20 min. Reprinted with permission from [243], Z. Fan, et al., Multifunctional plasmonic shell-magnetic core nanoparticles for targeted diagnostics, isolation, and photothermal destruction of tumor cells. *ACS Nano* 6, 1065 (2012). © 2012, American Chemistry Society.**

display magnetization and near-IR absorption.[240] Guo et al. have synthesized Fe_3O_4/Au hybrid nanostructures by means of 3-aminopropyltrimethoxysilane as a linker to adsorb Au nanoparticles, which also displayed near-IR absorption.[241] El-Sayed and coworkers have demonstrated that gold nanorods 20 nm in diameter and 78 nm in length have a longitudinal absorption mode in the NIR region and can also serve as a photothermal therapeutic agent.[47] The anti-HER2/neu-linked magnetic gold nanoshell fabricated by Hyeon et al.[242] for example, is a promising modality for targeted MRI and NIR photothermal therapy for cancer.

Fan et al.[243] reported the development of a MFMP core–shell nanotechnology-driven approach for the targeted diagnosis, isolation, and photothermal destruction of cancer cells. The aptamer-conjugated MFMP NPs can be used for targeted imaging and magnetic separation of a particular type of cells from a heterogeneous mixture of cancer cells (Fig. 15). A targeted photothermal experiment using 670 nm light at 2.5 W/cm^2 for 10 min resulted in selective irreparable cellular damage to most of the cancer cells. This aptamer-conjugated MFMP NP-based photothermal destruction of cancer cells was shown to be selective. The elegant multifunctional materials in biological systems inspire scientists to design analogous hierarchical structures with multifunctional capabilities characterized by surface-associated functions such as sensing, separation, and selective therapy.[221, 223, 244] Multifunctional material development is a key multidisciplinary and interdisciplinary field of the 21st century for biomedical imaging and novel therapeutics.[216–218]

Huang et al.[245] demonstrated that gold-nanoshell magnetic nanoeggs with surface-immobilized vancomycin (Van-Fe_3O_4@Au) are effective photothermal agents for the selective killing of pathogenic bacteria by means of illumination with NIR light. The temperature of a suspension of Van-Fe_3O_4@Au rises from 23 to approximately 55 °C during 3 min of illumination by NIR light. The cell growth of nosocomial pathogenic bacteria, including antibiotic-resistant strains, is targeted by the Van-Fe_3O_4@Au nanoeggs and can be effectively inhibited.

Ren et al.[246] demonstrated a facile method for synthesis of Fe_3O_4@Au NPs with biocompatibility via a self-assembly approach. The as-synthesized nanocomposites with average diameters of ca. 70 nm exhibit good biocompatibility, magnetic response, and optical properties. The Fe_3O_4@Au NPs can effectively convert NIR laser energy into heat. The sudden temperature increase leads to hyperthermia, rapidly causing cell death. Therefore, the fine-structured Fe_3O_4@Au NPs hold a great potential as a substrate of photothermal therapy with NIR laser irradiation.

SUMMARY AND PERSPECTIVE

Multifunctional magnetoplasmonic (MFMP) nanomaterials are proven platforms for biomedical applications due to their excellent surface chemistry and special optical and superparamagnetic properties. Several methods for synthesis of MFMP NPs with varied morphology have evolved in the past few decades. The multifunctional surfaces of MFMP NPs allow for rational conjugation of various biological and therapeutic molecules of interest. In the future, the ability to functionalize surfaces with molecules of varying nature and dimensions based on their means of attachment to cells—as well as the potential to shape the nanosurface physically, chemically, and topographically—will enable selective targeting of individual proteins and peptides within biological systems. Advancing the understanding of the influence of MFMP particle size, control of morphology, and the interfaces with cells is essential for the future development of nanotechnology and its biomedical applications. Such an interdisciplinary approach is complicated, therefore effective collaboration of scientists from different disciplines is necessary.

Acknowledgments: This study was supported by grants from the Korea Healthcare Technology R&D Project (A110191); by the Basic Science Research Program of the National Research Foundation of Korea (NRF) funded by the Ministry of Education (2013R1A1A4A010004637); and by the Civil and Military Technology Cooperation Program of the National Research Foundation of Korea (NRF) funded by the Ministry of Science, ICT and Future Planning (No. 2013M3C1A9055407).

REFERENCES

1. S. Hockfield, The next innovation revolution. *Science* 323, 1147 (**2009**).
2. H. L. Liu, C. H. Sonn, J. H. Wu, K. M. Lee, and Y. K. Kim, Synthesis of streptavidin-FITC-conjugated core–shell Fe_3O_4–Au nanocrystals and their application for the purification of CD4+ lymphocytes. *Biomaterials* 29, 4003 (**2008**).
3. S. Sun, C. B. Murray, D. Weller, L. Folks, and A. Moser, Monodisperse FePt nanoparticles and ferromagnetic FePt nanocrystal superlattices. *Science* 287, 1989 (**2000**).
4. J. Luo, L. Wang, D. Mott, P. N. Njoki, Y. Lin, T. He, Z. Xu, B. N. Wanjana, I. Lim, and S. Im, Core/shell nanoparticles as electrocatalysts for fuel cell reactions. *Adv. Mater.* 20, 4342 (**2008**).
5. C. Xu, J. Xie, D. Ho, C. Wang, N. Kohler, E. G. Walsh, J. R. Morgan, Y. E. Chin, and S. Sun, Au–Fe_3O_4 Dumbbell Nanoparticles as Dual-Functional Probes. *Angew. Chem. Int. Ed.* 47, 173 (**2008**).
6. J. H. Lee, Y. M. Huh, Y. w. Jun, J. w. Seo, J. t. Jang, H. T. Song, S. Kim, E. J. Cho, H. G. Yoon, and J. S. Suh, Artificially engineered magnetic nanoparticles for ultra-sensitive molecular imaging. *Nat. Med.* 13, 95 (**2006**).
7. W. J. Rieter, K. M. Taylor, H. An, W. Lin, and W. Lin, Nanoscale metal-organic frameworks as potential multimodal contrast enhancing agents. *J. Am. Chem. Soc.* 128, 9024 (**2006**).
8. J. Xie, F. Zhang, M. Aronova, L. Zhu, X. Lin, Q. Quan, G. Liu, G. Zhang, K. Y. Choi, and K. Kim, Manipulating the power of an additional phase: A flower-like Au–Fe_3O_4 optical nanosensor for imaging protease expressions *in vivo*. *ACS Nano* 5, 3043 (**2011**).
9. N. L. Rosi, D. A. Giljohann, C. S. Thaxton, A. K. Lytton-Jean, M. S. Han and C. A. Mirkin, Oligonucleotide-modified gold nanoparticles for intracellular gene regulation. *Science* 312, 1027 (**2006**).

10. D. A. Giljohann, D. S. Seferos, A. E. Prigodich, P. C. Patel, and C. A. Mirkin, Gene regulation with polyvalent siRNA-nanoparticle conjugates. *J. Am. Chem. Soc.* 131, 2072 (**2009**).
11. W. J. Rieter, K. M. Taylor, and W. Lin, Surface modification and functionalization of nanoscale metal-organic frameworks for controlled release and luminescence sensing. *J. Am. Chem. Soc.* 129, 9852 (**2007**).
12. C. Thomas, D. P. Ferris, J. H. Lee, E. Choi, M. H. Cho, E. S. Kim, J. F. Stoddart, J. S. Shin, J. Cheon, and J. I. Zink, Noninvasive remote-controlled release of drug molecules *in vitro* using magnetic actuation of mechanized nanoparticles. *J. Am. Chem. Soc.* 132, 10623 (**2010**).
13. M. S. Yavuz, Y. Cheng, J. Chen, C. M. Cobley, Q. Zhang, M. Rycenga, J. Xie, C. Kim, K. H. Song, and A. G. Schwartz, Gold nanocages covered by smart polymers for controlled release with near-infrared light. *Nat. Mater.* 8, 935 (**2009**).
14. C. Wang, C. Xu, H. Zeng, and S. Sun, Recent progress in syntheses and applications of dumbbell-like nanoparticles. *Adv. Mater.* 21, 3045 (**2009**).
15. S. E. Habas, H. Lee, V. Radmilovic, G. A. Somorjai, and P. Yang, Shaping binary metal nanocrystals through epitaxial seeded growth. *Nat. Mater.* 6, 692 (**2007**).
16. C. Wang, D. Van der Vliet, K. L. More, N. J. Zaluzec, S. Peng, S. Sun, H. Daimon, G. Wang, J. Greeley, and J. Pearson, Multimetallic Au/$FePt_3$ nanoparticles as highly durable electrocatalyst. *Nano. Lett.* 11, 919 (**2010**).
17. S. Vaidya, A. Kar, A. Patra, and A. K. Ganguli, Core–shell (CS) nanostructures and their application based on magnetic and optical properties. *Rev. Nanosci. Nanotechnol.* 2, 106 (**2013**).
18. C. Wang, H. Yin, S. Dai, and S. Sun, A general approach to noble metal–metal oxide dumbbell nanoparticles and their catalytic application for CO oxidation. *Chem. Mater.* 22, 3277 (**2010**).
19. D. K. Yi, S. T. Selvan, S. S. Lee, G. C. Papaefthymiou, D. Kundaliya, and J. Y. Ying, Silica-coated nanocomposites of magnetic nanoparticles and quantum dots. *J. Am. Chem. Soc.* 127, 4990 (**2005**).
20. H. S. Nalwa (ed.), Handbook of Nanostructured Materials and Nanotechnology, Academic Press, San Diego, CA (**2000**), Vols. 1–5.
21. H. S. Nalwa (ed.), Encyclopedia of Nanoscience and Nanotechnology, American Scientific Publishers, Los Angeles, CA (**2004/2011**), Vols. 1–25.
22. R. Elghanian, J. J. Storhoff, R. C. Mucic, R. L. Letsinger, and C. A. Mirkin, Selective colorimetric detection of polynucleotides based on the distance-dependent optical properties of gold nanoparticles. *Science* 277, 1078 (**1997**).
23. Y. Cui, Q. Wei, H. Park, and C. M. Lieber, Nanowire nanosensors for highly sensitive and selective detection of biological and chemical species. *Science* 293, 1289 (**2001**).
24. H. Gu, K. Xu, C. Xu, and B. Xu, Biofunctional magnetic nanoparticles for protein separation and pathogen detection. *Chem. Mater.* 941 (**2006**).
25. B. K. Bindhani, U. K. Parida, S. K. Biswal, A. K. Panigrahi, and P. L. Nayak, Gold nanoparticles and their biomedical applications. *Rev. Nanosci. Nanotechnol.* 2, 247 (**2013**).
26. S. E. Skrabalak, J. Chen, L. Au, X. Lu, X. Li, and Y. Xia, Gold nanocages for biomedical applications. *Adv. Mater.* 19, 3177 (**2007**).
27. J. Cheng, Y. J. Gu, S. H. Cheng, and W. T. Wong, Surface functionalized gold nanoparticles for drug delivery. *J. Biomed. Nanotechnol.* 9, 1362 (**2013**).
28. J. C. Love, L. A. Estroff, J. K. Kriebel, R. G. Nuzzo, and G. M. Whitesides, Self-assembled monolayers of thiolates on metals as a form of nanotechnology. *Chem. Rev.* 105, 1103 (**2005**).
29. M. C. Daniel and D. Astruc, Gold nanoparticles: Assembly, supramolecular chemistry, quantum-size-related properties, and applications toward biology, catalysis, and nanotechnology. *Chem. Rev.* 104, 293 (**2004**).
30. J. M. Nam, C. S. Thaxton, and C. A. Mirkin, Nanoparticle-based bio-bar codes for the ultrasensitive detection of proteins. *Science* 301, 1884 (**2003**).
31. A. Fu, C. M. Micheel, J. Cha, H. Chang, H. Yang, and A. P. Alivisatos, Discrete nanostructures of quantum dots/Au with DNA. *J. Am. Chem. Soc.* 126, 10832 (**2004**).
32. A. Riveros, K. Dadlani, E. Salas, L. Caballero, F. Melo, and M. J. Kogan, Gold nanoparticle-membrane interactions: Implications in biomedicine. *J. Biomater. Tissue. Eng.* 3, 4 (**2013**).
33. S. Laurent, D. Forge, M. Port, A. Roch, C. Robic, L. V. Elst, and R. N. Muller, Magnetic iron oxide nanoparticles: Synthesis, stabilization, vectorization, physicochemical characterizations, and biological applications. *Chem. Rev.* 108, 2064 (**2008**).
34. H. L. Liu, S. P. Ko, J. H. Wu, M. H. Jung, J. H. Min, J. H. Lee, B. H. An, and Y. K. Kim, One-pot polyol synthesis of monosize PVP-coated sub-5 nm Fe_3O_4 nanoparticles for biomedical applications. *J. Magn. Magn. Mater.* 310, e815 (**2007**).
35. S. R. Dave and X. Gao, Monodisperse magnetic nanoparticles for biodetection, imaging, and drug delivery: A versatile and evolving technology. *Wiley Interdiscip. Rev. Nanomed. Nanobiotechnol.* 1, 583 (**2009**).
36. C. M. Niemeyer, Nanoparticles, proteins, and nucleic acids: Biotechnology meets materials science. *Angew. Chem. Int. Ed.* 40, 4128 (**2001**).
37. J. Sangeetha, S. Thomas, J. Arutchelvi, M. Doble, and J. Philip, Functionalization of iron oxide nanoparticles with biosurfactants and biocompatibility studies. *J. Biomed. Nanotechnol.* 9, 751 (**2013**).
38. L. M. Demers, C. A. Mirkin, R. C. Mucic, R. A. Reynolds, R. L. Letsinger, R. Elghanian, and G. Viswanadham, A fluorescence-based method for determining the surface coverage and hybridization efficiency of thiol-capped oligonucleotides bound to gold thin films and nanoparticles. *Anal. Chem.* 72, 5535 (**2000**).
39. B. Ravel, E. E. Carpenter, and V. G. Harris, Oxidation of iron in iron/gold core/shell nanoparticles. *J. Appl. Phys.* 91, 8195 (**2002**).
40. J. Bao, W. Chen, T. Liu, Y. Zhu, P. Jin, L. Wang, J. Liu, Y. Wei, and Y. Li, Bifunctional Au–Fe_3O_4 nanoparticles for protein separation. *ACS Nano* 1, 293 (**2007**).
41. A. K. Gupta and M. Gupta, Synthesis and surface engineering of iron oxide nanoparticles for biomedical applications. *Biomaterials* 26, 3995 (**2005**).
42. S. J. Son, J. Reichel, B. He, M. Schuchman, and S. B. Lee, Magnetic nanotubes for magnetic-field-assisted bioseparation, biointeraction, and drug delivery. *J. Am. Chem. Soc.* 127, 7316 (**2005**).
43. S. Sieben, C. Bergemann, A. Lübbe, B. Brockmann, and D. Rescheleit, Comparison of different particles and methods for magnetic isolation of circulating tumor cells. *J. Magn. Magn. Mater.* 225, 175 (**2001**).
44. A.-H. Lu, E. L. Salabas, and F. Schüth, Magnetic nanoparticles: Synthesis, protection, functionalization, and application. *Angew. Chem. Int. Ed.* 46, 1222 (**2007**).
45. K. El-Boubbou, C. Gruden, and X. Huang, Magnetic glyconanoparticles: A unique tool for rapid pathogen detection, decontamination, and strain differentiation. *J. Am. Chem. Soc.* 129, 13392 (**2007**).
46. C. Sönnichsen, B. M. Reinhard, J. Liphardt, and A. P. Alivisatos, A molecular ruler based on plasmon coupling of single gold and silver nanoparticles. *Nat. Biotechnol.* 23, 741 (**2005**).
47. X. Huang, I. H. El-Sayed, W. Qian, and M. A. El-Sayed, Cancer cell imaging and photothermal therapy in the near-infrared region by using gold nanorods. *J. Am. Chem. Soc.* 128, 2115 (**2006**).
48. C. M. Pitsillides, E. K. Joe, X. Wei, R. Anderson, and C. P. Lin, Selective cell targeting with light-absorbing microparticles and nanoparticles. *Biophys. J.* 84, 4023 (**2003**).

49. L. Zhou, J. Yuan, and Y. Wei, Core–shell structural iron oxide hybrid nanoparticles: From controlled synthesis to biomedical applications. *J. Mater. Chem.* 21, 2823 **(2011)**.

50. L. Wang, H. Y. Park, S. I. I. Lim, M. J. Schadt, D. Mott, J. Luo, X. Wang, and C. J. Zhong, Core@shell nanomaterials: Gold-coated magnetic oxide nanoparticles. *J. Mater. Chem.* 18, 2629 **(2008)**.

51. R. Hao, R. Xing, Z. Xu, Y. Hou, S. Gao, and S. Sun, Synthesis, Functionalization, and biomedical applications of multifunctional magnetic nanoparticles. *Adv. Mater.* 22, 2729 **(2010)**.

52. H. Zeng and S. Sun, Syntheses, Properties, and potential applications of multicomponent magnetic nanoparticles. *Adv. Funct. Mater.* 18, 391 **(2008)**.

53. K. C.-F. Leung, S. Xuan, X. Zhu, D. Wang, C. P. Chak, S. F. Lee, W. K. W. Ho, and B. C. T. Chung, Gold and iron oxide hybrid nanocomposite materials. *Chem. Soc. Rev.* 41, 1911 **(2012)**.

54. S. J. Cho, J. C. Idrobo, J. Olamit, K. Liu, N. D. Browning, and S. M. Kauzlarich, Growth mechanisms and oxidation resistance of gold-coated iron nanoparticles. *Chem. Mater.* 17, 3181 **(2005)**.

55. J. L. Lyon, D. A. Fleming, M. B. Stone, P. Schiffer, and M. E. Williams, Synthesis of Fe oxide core/Au shell nanoparticles by iterative hydroxylamine seeding. *Nano Lett.* 4, 719 **(2004)**.

56. M. Mikhaylova, D. K. Kim, N. Bobrysheva, M. Osmolowsky, V. Semenov, T. Tsakalakos, and M. Muhammed, Superparamagnetism of magnetite nanoparticles: Dependence on surface modification. *Langmuir* 20, 2472 **(2004)**.

57. J. Zhang, M. Post, T. Veres, Z. J. Jakubek, J. Guan, D. Wang, F. Normandin, Y. Deslandes, and B. Simard, Laser-assisted synthesis of superparamagnetic Fe@Au core–shell nanoparticles. *J. Phys. Chem. B* 110, 7122 **(2006)**.

58. M. Spasova, V. Salgueiriño-Maceira, A. Schlachter, M. Hilgendorff, M. Giersig, L. M. Liz-Marzán, and M. Farle, Magnetic and optical tunable microspheres with a magnetite/gold nanoparticle shell. *J. Mater. Chem.* 15, 2095 **(2005)**.

59. W. R. Lee, M. G. Kim, J. R. Choi, J. I. Park, S. J. Ko, S. J. Oh, and J. Cheon, Redox-transmetalation process as a generalized synthetic strategy for core–shell magnetic nanoparticles. *J. Am. Chem. Soc.* 127, 16090 **(2005)**.

60. S. J. Cho, A. M. Shahin, G. J. Long, J. E. Davies, K. Liu, F. Grandjean, and S. M. Kauzlarich, Magnetic and Mössbauer spectral study of core/shell structured Fe/Au nanoparticles. *Chem. Mater.* 18, 960 **(2006)**.

61. J. Lim, A. Eggeman, F. Lanni, R. D. Tilton, and S. A. Majetich, Synthesis and single-particle optical detection of low-polydispersity plasmonic-superparamagnetic nanoparticles. *Adv. Mater.* 20, 1721 **(2008)**.

62. W. Schärtl, Crosslinked spherical nanoparticles with core–shell topology. *Adv. Mater.* 12, 1899 **(2000)**.

63. F. Caruso, Nanoengineering of particle surfaces. *Adv. Mater.* 13, 11 **(2001)**.

64. V. Skumryev, S. Stoyanov, Y. Zhang, G. Hadjipanayis, D. Givord, and J. Nogues, Beating the superparamagnetic limit with exchange bias. *Nature* 423, 850 **(2003)**.

65. H. Zeng, J. Li, Z. L. Wang, J. P. Liu, and S. Sun, Bimagnetic core/shell FePt/Fe_3O_4 nanoparticles. *Nano Lett.* 4, 187 **(2004)**.

66. J. Ge, Y. Hu, T. Zhang, and Y. Yin, Superparamagnetic composite colloids with anisotropic structures. *J. Am. Chem. Soc.* 129, 8974 **(2007)**.

67. H. Zhou, J. Lee, T. J. Park, S. J. Lee, J. Y. Park, and J. Lee, Ultrasensitive DNA monitoring by Au–Fe_3O_4 nanocomplex. *Sensor. Actuat. B-Chem.* 163, 224 **(2012)**.

68. Y. Cui, Y. Wang, W. Hui, Z. Zhang, X. Xin, and C. Chen, The synthesis of GoldMag nano-particles and their application for antibody immobilization. *Biomed. Microdevices* 7, 153 **(2005)**.

69. Z. Xu, Y. Hou, and S. Sun, Magnetic core/shell Fe_3O_4/Au and Fe_3O_4/Au/Ag nanoparticles with tunable plasmonic properties. *J. Am. Chem. Soc.* 129, 8698 **(2007)**.

70. W. Wu, Q. He, H. Chen, J. Tang, and L. Nie, Sonochemical synthesis, structure and magnetic properties of air-stable Fe_3O_4/Au nanoparticles. *Nanotechnology* 18, 145609 **(2007)**.

71. F. Bao, J. L. Yao, and R. A. Gu, Synthesis of magnetic Fe_2O_3/Au core/shell nanoparticles for bioseparation and immunoassay based on surface-enhanced Raman spectroscopy. *Langmuir* 25, 10782 **(2009)**.

72. E. Umut, F. Pineider, P. Arosio, C. Sangregorio, M. Corti, F. Tabak, A. Lascialfari, and P. Ghigna, Magnetic, optical and relaxometric properties of organically coated gold-magnetite (Au–Fe_3O_4) hybrid nanoparticles for potential use in biomedical applications. *J. Magn. Magn. Mater.* 324, 2373 **(2012)**.

73. G. Neri, A. Bonavita, C. Milone, and S. Galvagno, Role of the Au oxidation state in the CO sensing mechanism of Au/iron oxide-based gas sensors. *Sensor. Actuat. B-Chem.* 93, 402 **(2003)**.

74. C. B. Murray, C. R. Kagan, and M. G. Bawendi, Synthesis and characterization of monodisperse nanocrystals and close-packed nanocrystal assemblies. *Ann. Rev. Mater. Sci.* 30, 545 **(2000)**.

75. K. W. Kwon and M. Shim, γ-Fe_2O_3/II–VI sulfide nanocrystal heterojunctions. *J. Am. Chem. Soc.* 127, 10269 **(2005)**.

76. J. Gao, W. Zhang, P. Huang, B. Zhang, X. Zhang, and B. Xu, Intracellular spatial control of fluorescent magnetic nanoparticles. *J. Am. Chem. Soc.* 130, 3710 **(2008)**.

77. H. Yu, M. Chen, P. M. Rice, S. X. Wang, R. L. White, and S. Sun, Dumbbell-like bifunctional Au–Fe_3O_4 nanoparticles. *Nano Lett.* 5, 379 **(2005)**.

78. L. Lou, K. Yu, Z. Zhang, R. Huang, Y. Wang, and Z. Zhu, Facile methods for synthesis of core–shell structured and heterostructured Fe_3O_4@Au nanocomposites. *Appl. Surf. Sci.* 258, 8521 **(2012)**.

79. M. Wang, C. Wang, K. L. Young, L. Hao, M. Medved, T. Rajh, H. C. Fry, L. Zhu, G. S. Karczmar, and C. Watson, Cross-linked heterogeneous nanoparticles as bifunctional probe. *Chem. Mater.* 24, 2423 **(2012)**.

80. Y. Lee, M. A. Garcia, N. A. F. Huls, and S. Sun, Synthetic tuning of the catalytic properties of Au–Fe_3O_4 nanoparticles. *Angew. Chem.* 122, 1293 **(2010)**.

81. Y. S. Lin, S. H. Wu, Y. Hung, Y. H. Chou, C. Chang, M. L. Lin, C. P. Tsai, and C. Y. Mou, Multifunctional composite nanoparticles: Magnetic, luminescent, and mesoporous. *Chem. Mater.* 18, 5170 **(2006)**.

82. J. Lee, J. C. Park, J. U. Bang, and H. Song, Precise tuning of porosity and surface functionality in Au@SiO_2 nanoreactors for high catalytic efficiency. *Chem. Mater.* 20, 5839 **(2008)**.

83. A. Kumar, V. L. Pushparaj, S. Murugesan, G. Viswanathan, R. Nalamasu, R. J. Linhardt, O. Nalamasu, and P. M. Ajayan, Synthesis of silica-gold nanocomposites and their porous nanoparticles by an *in-situ* approach. *Langmuir* 22, 8631 **(2006)**.

84. F. Chen, Q. Chen, S. Fang, Y. Sun, Z. Chen, G. Xie, and Y. Du, Multifunctional nanocomposites constructed from Fe_3O_4–Au nanoparticle cores and a porous silica shell in the solution phase. *Dalton. Trans.* 40, 10857 **(2011)**.

85. H. Gu, Z. Yang, J. Gao, C. K. Chang, and B. Xu, Heterodimers of nanoparticles: Formation at a liquid–liquid interface and particle-specific surface modification by functional molecules. *J. Am. Chem. Soc.* 127, 34 **(2005)**.

86. X. F. Zhang, L. Clime, H. Q. Ly, M. Trudeau, and T. Veres, Multifunctional Fe_3O_4–Au/porous silica@fluorescein core/shell nanoparticles with enhanced fluorescence quantum yield. *J. Phys. Chem. C* 114, 18313 **(2010)**.

87. H. Xu, Y. S. Michael, E. Y. Wong, J. Uphoff, Y. Xu, J. A. Treadway, A. Truong, E. O'Brien, S. Asquith, and M. Stubbins, Multiplexed SNP genotyping using the Qbead™ system: A quantum dot-encoded microsphere-based assay. *Nucleic Acids Res.* 31, e43 **(2003)**.

88. Y. Xia, Y. Xiong, B. Lim, and S. E. Skrabalak, Shape-controlled synthesis of metal nanocrystals: Simple chemistry meets complex physics? *Angew. Chem. Int. Ed.* 48, 60 **(2009)**.

89. C. Burda, X. Chen, R. Narayanan, and M. A. El-Sayed, Chemistry and properties of nanocrystals of different shapes. *Chem. Rev.* 105, 1025 (**2005**).

90. J. Lee, H. Zhou, and J. Lee, Small molecule induced self-assembly of Au nanoparticles. *J. Mater. Chem.* 21, 16935 (**2011**).

91. N. Tian, Z. Y. Zhou, N. F. Yu, L. Y. Wang, and S. G. Sun, Direct electrodeposition of tetrahexahedral Pd nanocrystals with high-index facets and high catalytic activity for ethanol electrooxidation. *J. Am. Chem. Soc.* 132, 7580 (**2010**).

92. T. Ming, W. Feng, Q. Tang, F. Wang, L. Sun, J. Wang, and C. Yan, Growth of tetrahexahedral gold nanocrystals with high-index facets. *J. Am. Chem. Soc.* 131, 16350 (**2009**).

93. H. Y. Wu, M. Liu, and M. H. Huang, Direct synthesis of branched gold nanocrystals and their transformation into spherical nanoparticles. *J. Phys. Chem. B* 110, 19291 (**2006**).

94. C. S. Levin, C. Hofmann, T. A. Ali, A. T. Kelly, E. Morosan, P. Nordlander, K. H. Whitmire, and N. J. Halas, Magnetic-plasmonic core–shell nanoparticles. *ACS Nano* 3, 1379 (**2009**).

95. M. Yin and S. O'Brien, Synthesis of monodisperse nanocrystals of manganese oxides. *J. Am. Chem. Soc.* 125, 10180 (**2003**).

96. H. Zhou, J. P. Kim, J. H. Bahng, N. A. Kotov, and J. Lee, Self-assembly mechanism of spiky magnetoplasmonic supraparticles. *Adv. Funct. Mater.* 25, 1439 (**2014**).

97. S. Y. Zhu, L. L. Zhang, Q. Yu, T. Z. Wang, J. Chen, and M. X. Huo, Facile synthesis of a novel dendritic nanostructure of Fe_3O_4–Au nanorods. *Mater. Sci. Eng. B* 175, 172 (**2010**).

98. W. Hui, F. Shi, K. Yan, M. Peng, X. Cheng, Y. Luo, X. Chen, V. A. L. Roy, Y. Cui, and Z. Wang, Fe_3O_4/Au/Fe_3O_4 nanoflowers exhibiting tunable saturation magnetization and enhanced bioconjugation. *Nanoscale* 4, 747 (**2012**).

99. H. Zhu, E. Zhu, G. Ou, L. Gao, and J. Chen, Fe_3O_4–Au and Fe_2O_3–Au hybrid nanorods: Layer-by-layer assembly synthesis and their magnetic and optical properties. *Nanoscale. Res. Lett.* 5, 1755 (**2010**).

100. C. Wang, J. Chen, T. Talavage, and J. Irudayaraj, Gold Nanorod/Fe_3O_4 nanoparticle "nano-pearl-necklaces" for simultaneous targeting, dual-mode imaging, and photothermal ablation of cancer cells. *Angew. Chem.* 121, 2797 (**2009**).

101. S. Kameoka and A. P. Tsai, Alternately layered Au/Fe_3O_4 with porous structure-a self-assembled nanoarchitecture for catalysis materials. *J. Mater. Chem.* 20, 7348 (**2010**).

102. K. W. Chiu and J. J. Quinn, Magnetoplasma surface waves in metals. *Phys. Rev. B* 5, 4707 (**1972**).

103. E. D. Palik, R. Kaplan, R. W. Gammon, H. Kaplan, J. J. Quinn, and R. F. Wallis, Surface magnetoplasmon-optic phonon modes in InSb. *Phys. Lett. A* 45, 143 (**1973**).

104. W. Reim, O. E. Husser, J. Schoenes, E. Kaldis, P. Wachter, and K. Seiler, First magneto-optical observation of an exchange-induced plasma edge splitting. *J. Appl. Phys.* 55, 2155 (**1984**).

105. H. Feil and C. Haas, Magneto-optical Kerr effect, enhanced by the plasma resonance of charge carriers. *Phys. Rev. Lett.* 58, 65 (**1987**).

106. P. H. Damgaard and U. M. Heller, Observation of the meissner effect in a lattice higgs model. *Phys. Rev. Lett.* 60, 1246 (**1988**).

107. R. Nies and F. R. Kessler, Comment on enhancement of the magneto-optical Kerr rotation in Fe/Cu bilayered films. *Phys. Rev. Lett.* 64, 105 (**1990**).

108. W. Reim and D. Weller, Kerr rotation enhancement in metallic bilayer thin films for magneto-optical recording. *Appl. Phys. Lett.* 53, 2453 (**1988**).

109. W. A. McGahan, L.-Y. Chen, Z. S. Shan, D. J. Sellmyer, and J. A. Woollam, Enhanced magneto-optic Kerr effects in thin magnetic/metallic layered structures. *Appl. Phys. Lett.* 55, 2479 (**1989**).

110. V. I. Safarov, V. A. Kosobukin, C. Hermann, G. Lampel, J. Peretti, and C. Marliere, Magneto-optical effects enhanced by surface plasmons in metallic multilayer films. *Phys. Rev. Lett.* 73, 3584 (**1994**).

111. C. Hermann, V. A. Kosobukin, G. Lampel, J. Peretti, V. I. Safarov, and P. Bertrand, Surface-enhanced magneto-optics in metallic multilayer films. *Phys. Rev. B* 64, 235422 (**2001**).

112. S. Y. Wang, W. M. Zheng, D. L. Qian, R. J. Zhang, Y. X. Zheng, S. M. Zhou, Y. M. Yang, B. Y. Li, and L. Y. Chen, Study of the Kerr effect of granular films. *J. Appl. Phys.* 85, 5121 (**1999**).

113. W. M. Zheng, L. Y. Chen, and J. H. Chu, The Magneto-optical Kerr effect enhancement in CoxAg1-*x* granular films. *Phys. Status. Solidi. B* 214, 463 (**1999**).

114. W. M. Zheng, S. Y. Wang, D. L. Qian, Y. X. Zheng, Y. M. Yang, B. Y. Li and L. Y. Chen, The magneto-optical properties of Co–Ag granular films. *J. Magn. Magn. Mater.* 198–199, 210 (**1999**).

115. J. Yue, X. Jiang, and A. Yu, Molecular dynamics study on Au/Fe_3O_4 nanocomposites and their surface function toward amino acids. *J. Phys. Chem. B* 115, 11693 (**2011**).

116. W. Brullot, V. K. Valev, and T. Verbiest, Magnetic-plasmonic nanoparticles for the life sciences: Calculated optical properties of hybrid structures. *Nanomedicine* 8, 559 (**2012**).

117. G. Armelles, A. Cebollada, A. García-Martín, J. M. García-Martín, M. U. González, J. B. González-Díaz, E. Ferreiro-Vila, and J. F. Torrado, Magnetoplasmonic nanostructures: Systems supporting both plasmonic and magnetic properties. *J. Opt. A* 11, 114023 (**2009**).

118. G. Armelles, A. Cebollada, A. García-Martín, and M. U. González, Magnetoplasmonics: Combining magnetic and plasmonic functionalities. *Adv. Opt. Mater.* 1, 10 (**2013**).

119. S. Melle, J. L. Menendez, G. Armelles, D. Navas, M. Vazquez, K. Nielsch, R. B. Wehrspohn, and U. Gosele, Magneto-optical properties of nickel nanowire arrays. *Appl. Phys. Lett.* 83, 4547 (**2003**).

120. A. Batalov, C. Zierl, T. Gaebel, P. Neumann, I. Y. Chan, G. Balasubramanian, P. R. Hemmer, F. Jelezko, and J. Wrachtrup, Temporal coherence of photons emitted by single nitrogen-vacancy defect centers in diamond using optical Rabi-oscillations. *Phys. Rev. Lett.* 100, 077401 (**2008**).

121. Z. Liu, L. Shi, Z. Shi, X. H. Liu, J. Zi, S. M. Zhou, S. J. Wei, J. Li, X. Zhang, and Y. J. Xia, Magneto-optical Kerr effect in perpendicularly magnetized Co/Pt films on two-dimensional colloidal crystals. *Appl. Phys. Lett.* 95, 032502 (**2009**).

122. G. Ctistis, E. Papaioannou, P. Patoka, J. Gutek, P. Fumagalli, and M. Giersig, Optical and magnetic properties of hexagonal arrays of subwavelength holes in optically thin cobalt films. *Nano. Lett.* 9, 1 (**2008**).

123. V. Bonanni, S. Bonetti, T. Pakizeh, Z. Pirzadeh, J. Chen, J. Nogués, P. Vavassori, R. Hillenbrand, J. Åkerman, and A. Dmitriev, Designer magnetoplasmonics with nickel nanoferromagnets. *Nano Lett.* 11, 5333 (**2011**).

124. J. Chen, P. Albella, Z. Pirzadeh, P. Alonso-González, F. Huth, S. Bonetti, V. Bonanni, J. Åkerman, J. Nogués, and P. Vavassori, Plasmonic nickel nanoantennas. *Small* 7, 2341 (**2011**).

125. J. B. González-Díaz, A. García-Martín, J. M. García-Martín, A. Cebollada, G. Armelles, B. Sepúveda, Y. Alaverdyan, and M. Käll, Plasmonic Au/Co/Au nanosandwiches with enhanced magneto-optical activity. *Small* 4, 202 (**2008**).

126. T. Katayama, Y. Suzuki, H. Awano, Y. Nishihara, and N. Koshizuka, Enhancement of the magneto-optical Kerr rotation in Fe/Cu bilayered films. *Phys. Rev. Lett.* 60, 1426 (**1988**).

127. J. B. Gonzelez-Diaz, B. Sepulveda, A. Garcia-Martin, and G. Armelles, Cobalt dependence of the magneto-optical response in magnetoplasmonic nanodisks. *Appl. Phys. Lett.* 97, 043114 (**2010**).

128. J. C. Banthí, D. Meneses-Rodríguez, F. García, M. U. González, A. García-Martín, A. Cebollada, and G. Armelles, High magneto-optical activity and low optical losses in metal-dielectric Au/Co/Au–SiO_2 magnetoplasmonic nanodisks. *Adv. Mater.* 24, OP36 (**2012**).

129. V. V. Temnov, G. Armelles, U. Woggon, D. Guzatov, A. Cebollada, A. Garcia-Martin, J. M. Garcia-Martin, T. Thomay,

A. Leitenstorfer, and R. Bratschitsch, Active magneto-plasmonics in hybrid metal-ferromagnet structures. *Nat. Photonics* 4, 107 **(2010)**.

130. A. García-Martín, G. Armelles, and S. Pereira, Light transport in photonic crystals composed of magneto-optically active materials. *Phys. Rev. B* 71, 205116 **(2005)**.

131. N. Bonod, R. Reinisch, E. Popov, and M. Nevière, Optimization of surface-plasmon-enhanced magneto-optical effects. *J. Opt. Soc. Am. B* 21, 791 **(2004)**.

132. B. I. Khudik, V. Z. Lozovskii, and I. V. Nazarenko-Bary Akhtar, Macroscopic electrodynamics of ultra-thin films. *Phys. Status Solidi. B* 153, 167 **(1989)**.

133. M. L. Bah, A. Akjouj, and L. Dobrzynski, Response functions in layered dielectric media. *Surf. Sci. Rep.* 16, 97 **(1992)**.

134. O. Keller, Local fields in the electrodynamics of mesoscopic media. *Phys. Rep.* 268, 85 **(1996)**.

135. S. A. Maier and H. A. Atwater, Plasmonics: Localization and guiding of electromagnetic energy in metal/dielectric structures. *J. Appl. Phys.* 98, 011101 **(2005)**.

136. S. Kawata, M. Ohtsu, M. Irie, and Masahiro (eds.), Near-Field Optics and Surface Plasmon Polaritons, Springer, New York **(2001)**, Vols. 1–81.

137. D. Beddows, B. C. Griffiths, O. Samek, and H. H. Telle, Application of frustrated total internal reflection devices to analytical laser spectroscopy. *Appl. Opt.* 42, 6006 **(2003)**.

138. B. Sepúlveda, L. G. Carrascosa, D. Regatos, M. A. Otte, D. Farina, and L. M. Lechuga, Surface plasmon resonance biosensors for highly sensitive detection in real samples, *Proc. SPIE*, International Society for Optics and Photonics, San Diego, CA **(2009)**, p. 73970Y.

139. V. Chegel, Y. Chegel, M. D. Guiver, A. Lopatynskyi, O. Lopatynska, and V. Lozovski, 3D-quantification of biomolecular covers using surface plasmon-polariton resonance experiment. *Sens. Actuator B-Chem.* 134, 66 **(2008)**.

140. B. Sepúlveda, P. C. Angelomé, L. M. Lechuga, and L. M. Liz-Marzán, LSPR-based nanobiosensors. *Nano Today* 4, 244 **(2009)**.

141. D. P. O'Neal, L. R. Hirsch, N. J. Halas, J. D. Payne, and J. L. West, Photo-thermal tumor ablation in mice using near infrared-absorbing nanoparticles. *Cancer Lett.* 209, 171 **(2004)**.

142. G. K. Kouassi and J. Irudayaraj, Magnetic and gold-coated magnetic nanoparticles as a DNA sensor. *Anal. Chem.* 78, 3234 **(2006)**.

143. B. Dubertret, P. Skourides, D. J. Norris, V. Noireaux, A. H. Brivanlou, and A. Libchaber, *In vivo* imaging of quantum dots encapsulated in phospholipid micelles. *Science* 298, 1759 **(2002)**.

144. J. Salado, M. Insausti, L. Lezama, I. G. de Muro, M. Moros, B. Pelaz, V. Grazu, J. M. de la Fuente, and T. Rojo, Functionalized Fe_3O_4@Au superparamagnetic nanoparticles: *In vitro* bioactivity. *Nanotechnology* 23, 315102 **(2012)**.

145. X. Chao, F. Shi, Y. Y. Zhao, K. Li, M. L. Peng, C. Chen, and Y. L. Cui, Cytotoxicity of Fe_3O_4/Au composite nanoparticles loaded with doxorubicin combined with magnetic field. *Die. Pharmazie* 65, 500 **(2010)**.

146. J. Della Rocca, D. Liu, and W. Lin, Nanoscale metal-organic frameworks for biomedical imaging and drug delivery. *Acc. Chem. Res.* 44, 957 **(2011)**.

147. N. Ma, C. Ma, C. Li, T. Wang, Y. Tang, H. Wang, X. Mou, Z. Chen, and N. He, Influence of nanoparticle shape, size, and surface functionalization on cellular uptake. *J. Nanosci. Nanotechnol.* 13, 6485 **(2013)**.

148. D. R. Absolom, W. Zingg, and A. W. Neumann, Protein adsorption to polymer particles: Role of surface properties. *J. Biomed. Mater. Res.* 21, 161 **(1987)**.

149. Z. Xu, L. Chen, W. Gu, Y. Gao, L. Lin, Z. Zhang, Y. Xi, and Y. Li, The performance of docetaxel-loaded solid lipid nanoparticles targeted to hepatocellular carcinoma. *Biomaterials* 30, 226 **(2009)**.

150. B. D. Chithrani, A. A. Ghazani, and W. C. Chan, Determining the size and shape dependence of gold nanoparticle uptake into mammalian cells. *Nano Lett.* 6, 662 **(2006)**.

151. S. E. Gratton, P. A. Ropp, P. D. Pohlhaus, J. C. Luft, V. J. Madden, M. E. Napier, and J. M. DeSimone, The effect of particle design on cellular internalization pathways. *Proc. Natl. Acad. Sci.* 105, 11613 **(2008)**.

152. Y. Li, J. Liu, Y. Zhong, J. Zhang, Z. Wang, L. Wang, Y. An, M. Lin, Z. Gao, and D. Zhang, Biocompatibility of Fe_3O_4@ Au composite magnetic nanoparticles *in vitro* and *in vivo*. *Int. J. Nanomedicine.* 6, 2805 **(2011)**.

153. M. P. Melancon, W. Lu, and C. Li, Gold-based magneto/optical nanostructures: Challenges for *in vivo* applications in cancer diagnostics and therapy. *MRS. Bull.* 34, 415 **(2009)**.

154. J. H. Heo, K. I. Kim, M. H. Lee, and J. H. Lee, Stability of a gold nanoparticle-DNA system in seawater. *J. Nanosci. Nanotechnol.* 13, 7254 **(2013)**.

155. L. L. Pang, J. S. Li, J. H. Jiang, Y. Le, G. L. Shen, and R. Q. Yu, A novel detection method for DNA point mutation using QCM based on Fe_3O_4/Au core/shell nanoparticle and DNA ligase reaction. *Sens. Actuator B-Chem.* 127, 311 **(2007)**.

156. A. Yu, T. Geng, Q. Fu, C. Chen, and Y. Cui, Biotin-avidin amplified magnetic immunoassay for hepatitis B surface antigen detection using GoldMag nanoparticles. *J. Magn. Magn. Mater.* 311, 421 **(2007)**.

157. X. Zhou, W. Xu, Y. Wang, Q. Kuang, Y. Shi, L. Zhong, and Q. Zhang, Fabrication of cluster/shell Fe_3O_4/Au nanoparticles and application in protein detection via a SERS method. *J. Phys. Chem. C* 114, 19607 **(2010)**.

158. L. Zhang, J. Xu, L. Mi, H. Gong, S. Jiang, and Q. Yu, Multifunctional magnetic-plasmonic nanoparticles for fast concentration and sensitive detection of bacteria using SERS. *Biosens. Bioelectron.* 31, 130 **(2012)**.

159. X. Wang, L. Wei, G. Tao, and L. Dai, Determination of hydrocortisone in cosmetics by CdSe/CdS quantum dots-based fluoroimmunoassay using magnetic Fe_3O_4/Au nanoparticles as solid carriers. *Chin. J. Chem.* 29, 587 **(2011)**.

160. H. Zhou, J. Dong, V. K. Deo, E. Y. Park, and J. Lee, Detection of anti-neospora antibodies in bovine serum by using Spiky Au–CdTe nanocomplexes. *Sens. Actuator B-Chem.* 178, 192 **(2012)**.

161. J. D. Qiu, M. Xiong, R. P. Liang, H. P. Peng, and F. Liu, Synthesis and characterization of ferrocene modified Fe_3O_4@Au magnetic nanoparticles and its application. *Biosens. Bioelectron.* 24, 2649 **(2009)**.

162. N. Gan, H. Jin, T. Li, and L. Zheng, Fe_3O_4/Au magnetic nanoparticle amplification strategies for ultrasensitive electrochemical immunoassay of alfa-fetoprotein. *Int. J. Nanomedicine* 6, 3259 **(2011)**.

163. L. Lou, K. Yu, Z. Zhang, R. Huang, J. Zhu, Y. Wang, and Z. Zhu, Dual-mode protein detection based on Fe_3O_4–Au hybrid nanoparticles. *Nano. Res.* 5, 272 **(2012)**.

164. L. He, E. A. Smith, M. J. Natan, and C. D. Keating, The distance-dependence of colloidal Au-amplified surface plasmon resonance. *J. Phys. Chem. B* 108, 10973 **(2004)**.

165. Y. Teramura and H. Iwata, Label-free immunosensing for α-fetoprotein in human plasma using surface plasmon resonance. *Anal. Biochem.* 365, 201 **(2007)**.

166. Y. Sato, K. Fujimoto, and H. Kawaguchi, Detection of a *K*-ras point mutation employing peptide nucleic acid at the surface of a SPR biosensor. *Colloid. Surf. B-Biointerfaces* 27, 23 **(2003)**.

167. J. Treviño, A. Calle, J. M. Rodríguez-Frade, M. Mellado, and L. M. Lechuga, Determination of human growth hormone in human serum samples by surface plasmon resonance immunoassay. *Talanta* 78, 1011 **(2009)**.

168. V. Chabot, C. M. Cuerrier, E. Escher, V. Aimez, M. Grandbois, and P. G. Charette, Biosensing based on surface plasmon resonance and living cells. *Biosens. Bioelectron.* 24, 1667 **(2009)**.

169. J. Ladd, H. Lu, A. D. Taylor, V. Goodell, M. L. Disis, and S. Jiang, Direct detection of carcinoembryonic antigen autoantibodies in clinical human serum samples using a surface plasmon resonance sensor. *Colloid. Surf. B-Biointerfaces* 70, 1 **(2009)**.

170. J. Wang, A. Munir, Z. Li, and H. S. Zhou, Aptamer-Au NPs conjugates-enhanced SPR sensing for the ultrasensitive sandwich immunoassay. *Biosens. Bioelectron.* 25, 124 **(2009)**.

171. Y. Sun, Y. Bai, D. Song, X. Li, L. Wang, and H. Zhang, Design and performances of immunoassay based on SPR biosensor with magnetic microbeads. *Biosens. Bioelectron.* 23, 473 **(2007)**.

172. D. Yang, J. Ma, M. Peng, Q. Zhang, Y. Luo, W. Hui, T. Jin, and Y. Cui, Building NanoSPR biosensor systems based on gold magnetic composite nanoparticles. *J. Nanosci. Nanotechnol.* 13, 5485 **(2013)**.

173. R. P. Liang, G. H. Yao, L. X. Fan, and J. D. Qiu, Magnetic Fe_3O_4@Au composite-enhanced surface plasmon resonance for ultrasensitive detection of magnetic nanoparticle-enriched α-fetoprotein. *Anal. Chim. Acta* 737, 22 **(2012)**.

174. J. Wang, Y. Sun, L. Wang, X. Zhu, H. Zhang, and D. Song, Surface plasmon resonance biosensor based on Fe_3O_4/Au nanocomposites. *Colloid. Surf. B-Biointerfaces* 81, 600 **(2010)**.

175. H. Zhang, Y. Sun, J. Wang, J. Zhang, H. Zhang, H. Zhou, and D. Song, Preparation and application of novel nanocomposites of magnetic-Au nanorod in SPR biosensor. *Biosens. Bioelectron.* 34, 137 **(2012)**.

176. J. Kim, H.-Y. Park, J. Kim, J. Ryu, Y. D. Kwon, R. Grailhe, and R. Song, Ni-nitrilotriacetic acid-modified quantum dots as a site-specific labeling agent of histidine-tagged proteins in live cells. *Chem. Commun.* 16, 1910 **(2008)**.

177. R. Ahrends, S. Pieper, B. Neumann, C. Scheler, and M. W. Linscheid, Metal-coded affinity tag labeling: A demonstration of analytical robustness and suitability for biological applications. *Anal. Chem.* 81, 2176 **(2009)**.

178. R. Ahrends, S. Pieper, A. Kühn, H. Weisshoff, M. Hamester, T. Lindemann, C. Scheler, K. Lehmann, K. Taubner, and M. W. Linscheid, A metal-coded affinity tag approach to quantitative proteomics. *Mol. Cell. Proteomics* 6, 1907 **(2007)**.

179. S. H. Kim, M. Jeyakumar, and J. A. Katzenellenbogen, Dual-mode fluorophore-doped nickel nitrilotriacetic acid-modified silica nanoparticles combine histidine-tagged protein purification with site-specific fluorophore labeling. *J. Am. Chem. Soc.* 129, 13254 **(2007)**.

180. M. Hu, J. Chen, Z. Y. Li, L. Au, G. V. Hartland, X. Li, M. Marquez, and Y. Xia, Gold nanostructures: Engineering their plasmonic properties for biomedical applications. *Chem. Soc. Rev.* 35, 1084 **(2006)**.

181. S. J. Hurst, M. S. Han, A. K. R. Lytton-Jean, and C. A. Mirkin, Screening the sequence selectivity of DNA-binding molecules using a gold nanoparticle-based colorimetric approach. *Anal. Chem.* 79, 7201 **(2007)**.

182. I. Willner, R. Baron, and B. Willner, Integrated nanoparticle-biomolecule systems for biosensing and bioelectronics. *Biosens. Bioelectron.* 22, 1841 **(2007)**.

183. G. Shen, H. wang, G. Shen, and R. Yu, Au nanoparticle network-type thin films formed via mixed assembling and cross-linking route for biosensor application: Quartz crystal microbalance study. *Anal. Biochem.* 365, 1 **(2007)**.

184. K. Kamei, Y. Mukai, H. Kojima, T. Yoshikawa, M. Yoshikawa, G. Kiyohara, T. A. Yamamoto, Y. Yoshioka, N. Okada, S. Seino, and S. Nakagawa, Direct cell entry of gold/iron-oxide magnetic nanoparticles in adenovirus mediated gene delivery. *Biomaterials* 30, 1809 **(2009)**.

185. H. Y. Park, M. J. Schadt, Wang, I. I. S. Lim, P. N. Njoki, S. H. Kim, M. Y. Jang, J. Luo, and C. J. Zhong, Fabrication of Magnetic Core@Shell Fe Oxide@Au Nanoparticles for Interfacial Bioactivity and Bio-separation. *Langmuir* 23, 9050 **(2007)**.

186. T. Pellegrino, A. Fiore, E. Carlino, C. Giannini, P. D. Cozzoli, G. Ciccarella, M. Respaud, L. Palmirotta, R. Cingolani, and L. Manna, Heterodimers based on $CoPt_3$–Au nanocrystals with tunable domain size. *J. Am. Chem. Soc.* 128, 6690 **(2006)**.

187. H. Y. Xie, R. Zhen, B. Wang, Y. J. Feng, P. Chen, and J. Hao, Fe_3O_4/Au core/shell nanoparticles modified with Ni2+-nitrilotriacetic acid specific to histidine-tagged proteins. *J. Phys. Chem. C* 114, 4825 **(2010)**.

188. I. I. Lim, P. N. Njoki, H. Y. Park, X. Wang, L. Wang, D. Mott, and C. J. Zhong, Gold and magnetic oxide/gold core/shell nanoparticles as bio-functional nanoprobes. *Nanotechnology* 19, 305102 **(2008)**.

189. J. Jeong, T. H. Ha, and B. H. Chung, Enhanced reusability of hexa-arginine-tagged esterase immobilized on gold-coated magnetic nanoparticles. *Anal. Chim. Acta* 569, 203 **(2006)**.

190. S. Qiu, L. Xu, Y. R. Cui, Q. P. Deng, W. Wang, H. X. Chen, and X. X. Zhang, Pseudo-homogeneous immunoextraction of epitestosterone from human urine samples based on gold-coated magnetic nanoparticles. *Talanta* 81, 819 **(2010)**.

191. Y. R. Cui, C. Hong, Y. L. Zhou, Y. Li, X. M. Gao, and X. X. Zhang, Synthesis of orientedly bioconjugated core/shell Fe_3O_4@Au magnetic nanoparticles for cell separation. *Talanta* 85, 1246 **(2011)**.

192. J. S. Xu, J. Huang, R. Qin, G. H. Hinkle, S. P. Povoski, E. W. Martin and R. X. Xu, Synthesizing and binding dual-mode poly (lactic-co-glycolic acid) (PLGA) nanobubbles for cancer targeting and imaging. *Biomaterials* 31, 1716 **(2010)**.

193. G. Zhang, X. Zeng, and P. Li, Nanomaterials in cancer-therapy drug delivery system. *J. Biomed. Nanotechnol.* 9, 741 **(2013)**.

194. H. S. Nalwa and T. Webster (eds.), Cancer Nanotechnology: Nanomaterials for Cancer Diagnosis and Therapy, American Scientific Publishers, Los Angeles, CA **(2007)**.

195. B. Sitharaman, K. R. Kissell, K. B. Hartman, L. A. Tran, A. Baikalov, I. Rusakova, Y. Sun, H. A. Khant, S. J. Ludtke, W. Chiu, S. Laus, E. Toth, L. Helm, A. E. Merbach, and L. J. Wilson, Superparamagnetic gadonanotubes are high-performance MRI contrast agents. *Chem. Commun.* 31, 3915 **(2005)**.

196. S. Ahn, S. Y. Jung, J. P. Lee, H. K. Kim, and S. J. Lee, Gold nanoparticle flow sensors designed for dynamic X-ray imaging in biofluids. *ACS Nano* 4, 3753 **(2010)**.

197. P. Diagaradjane, A. Deorukhkar, J. G. Gelovani, D. M. Maru, and S. Krishnan, Gadolinium chloride augments tumor-specific imaging of targeted quantum dots *in vivo*. *ACS Nano* 4, 4131 **(2010)**.

198. J. Kim, Y. Piao, and T. Hyeon, Multifunctional nanostructured materials for multimodal imaging, and simultaneous imaging and therapy. *Chem. Soc. Rev.* 38, 372 **(2009)**.

199. H. Y. Ko, K. J. Choi, C. H. Lee, and S. Kim, A multimodal nanoparticle-based cancer imaging probe simultaneously targeting nucleolin, integrin $\alpha_v\beta_3$ and tenascin-C proteins. *Biomaterials* 32, 1130 **(2011)**.

200. B. Chen, H. Zhang, C. Zhai, N. Du, C. Sun, J. Xue, D. Yang, H. Huang, B. Zhang, Q. Xie, and Y. Wu, Carbon nanotube-based magnetic-fluorescent nanohybrids as highly efficient contrast agents for multimodal cellular imaging. *J. Mater. Chem.* 20, 9895 **(2010)**.

201. H. K. Kim, H. Y. Jung, J. A. Park, M. I. Huh, J. C. Jung, Y. Chang, and T. J. Kim, Gold nanoparticles coated with gadolinium-DTPA-bisamide conjugate of penicillamine (Au@GdL) as a T1-weighted blood pool contrast agent. *J. Mater. Chem.* 20, 5411 **(2010)**.

202. M. Kacenka, O. Kaman, J. Kotek, L. Falteisek, J. Cerny, D. Jirak, V. Herynek, K. Zacharovova, Z. Berkova, P. Jendelova, J. Kupcik, E. Pollert, P. Veverka, and I. Lukes, Dual imaging probes for magnetic resonance imaging and fluorescence microscopy based on perovskite manganite nanoparticles. *J. Mater. Chem.* 21, 157 **(2011)**.

203. S. T. Selvan, P. K. Patra, C. Y. Ang, and J. Y. Ying, Synthesis of silica-coated semiconductor and magnetic quantum dots and their use in the imaging of live cells. *Angew. Chem.* 119, 2500 **(2007)**.

204. W. J. M. Mulder, G. J. Strijkers, G. A. F. van Tilborg, A. W. Griffioen and K. Nicolay, Lipid-based nanoparticles for contrast-enhanced MRI and molecular imaging. *NMR Biomed.* 19, 142 **(2006)**.

205. J. Yang, E. K. Lim, H. J. Lee, J. Park, S. C. Lee, K. Lee, H. G. Yoon, J. S. Suh, Y. M. Huh, and S. Haam, Fluorescent magnetic nanohybrids as multimodal imaging agents for human epithelial cancer detection. *Biomaterials* 29, 2548 **(2008)**.

206. P. Sharma, S. C. Brown, N. Bengtsson, Q. Zhang, G. A. Walter, S. R. Grobmyer, S. Santra, H. Jiang, E. W. Scott, and B. M. Moudgil, Gold-speckled multimodal nanoparticles for noninvasive bioimaging. *Chem. Mater.* 20, 6087 **(2008)**.

207. F. Bertorelle, C. Wilhelm, J. Roger, F. Gazeau, C. Ménager, and V. Cabuil, Fluorescence-modified superparamagnetic nanoparticles: Intracellular uptake and use in cellular imaging. *Langmuir* 22, 5385 **(2006)**.

208. L. Moriggi, C. Cannizzo, E. Dumas, C. R. Mayer, A. Ulianov, and L. Helm, Gold nanoparticles functionalized with gadolinium chelates as high-relaxivity MRI contrast agents. *J. Am. Chem. Soc.* 131, 10828 **(2009)**.

209. G. Zhang, Z. Yang, W. Lu, R. Zhang, Q. Huang, M. Tian, L. Li, D. Liang and C. Li, Influence of anchoring ligands and particle size on the colloidal stability and *in vivo* biodistribution of polyethylene glycol-coated gold nanoparticles in tumor-xenografted mice. *Biomaterials* 30, 1928 **(2009)**.

210. P. J. Chen, S. H. Hu, C. S. Hsiao, Y. Y. Chen, D. M. Liu, and S. Y. Chen, Multifunctional magnetically removable nanogated lids of Fe_3O_4-capped mesoporous silica nanoparticles for intracellular controlled release and MR imaging. *J. Mater. Chem.* 21, 2535 **(2011)**.

211. D. A. Giljohann, D. S. Seferos, W. L. Daniel, M. D. Massich, P. C. Patel, and C. A. Mirkin, Gold nanoparticles for biology and medicine. *Angew. Chem. Int. Ed.* 49, 3280 **(2010)**.

212. R. Popovtzer, A. Agrawal, N. A. Kotov, A. Popovtzer, J. Balter, T. Carey, and R. Kopelman, Targeted gold nanoparticles enable molecular CT imaging of cancer. *Nano Lett.* 8, 4593 **(2008)**.

213. T. Zhou, B. Wu, and D. Xing, Bio-modified Fe_3O_4 core/Au shell nanoparticles for targeting and multimodal imaging of cancer cells. *J. Mater. Chem.* 22, 470 **(2012)**.

214. H. Cai, K. Li, M. Shen, S. Wen, Y. Luo, C. Peng, G. Zhang, and X. Shi, Facile assembly of Fe_3O_4@ Au nanocomposite particles for dual mode magnetic resonance and computed tomography imaging applications. *J. Mater. Chem.* 22, 15110 **(2012)**.

215. S. Narayanan, B. N. Sathy, U. Mony, M. Koyakutty, S. V. Nair, and D. Menon, Biocompatible magnetite/gold nanohybrid contrast agents via green chemistry for MRI and CT bioimaging. *ACS Appl. Mater. Interfaces.* 4, 251 **(2011)**.

216. W. Lu, A. K. Singh, S. A. Khan, D. Senapati, H. Yu, and P. C. Ray, Gold nano-popcorn-based targeted diagnosis, nanotherapy treatment, and *in situ* monitoring of photothermal therapy response of prostate cancer cells using surface-enhanced raman spectroscopy. *J. Am. Chem. Soc.* 132, 18103 **(2010)**.

217. M. Ljungman, Targeting the DNA damage response in cancer. *Chem. Rev.* 109, 2929 **(2009)**.

218. M. Ferrari, Cancer nanotechnology: Opportunities and challenges. *Nat. Rev. Cancer* 5, 161 **(2005)**.

219. D. A. Scheinberg, C. H. Villa, F. E. Escorcia, and M. R. McDevitt, Conscripts of the infinite armada: Systemic cancer therapy using nanomaterials. *Nat. Rev. Clin. Oncol.* 7, 266 **(2010)**.

220. P. K. Jain, X. Huang, I. H. El-Sayed, and M. A. El-Sayed, Noble metals on the nanoscale: Optical and photothermal properties and some applications in imaging, sensing, biology, and medicine. *Acc. Chem. Res.* 41, 1578 **(2008)**.

221. S. Lal, S. E. Clare, and N. J. Halas, Nanoshell-enabled photothermal cancer therapy: Impending clinical impact. *Acc. Chem. Res.* 41, 1842 **(2008)**.

222. R. Bardhan, S. Lal, A. Joshi, and N. J. Halas, Theranostic nanoshells: From probe design to imaging and treatment of cancer. *Acc. Chem. Res.* 44, 936 **(2011)**.

223. J. Gao, H. Gu, and B. Xu, Multifunctional magnetic nanoparticles: Design, synthesis, and biomedical applications. *Acc. Chem. Res.* 42, 1097 **(2009)**.

224. N. Chanda, A. Upendran, E. J. Boote, A. Zambre, S. Axiak, K. Selting, K. V. Katti, W. M. Leevy, Z. Afrasiabi, J. Vimal, J. Singh, J. C. Lattimer and R. Kannan, Gold nanoparticle based X-ray contrast agent for tumor imaging in mice and dog: A potential nanoplatform for computer tomography theranostics. *J. Biomed. Nanotechnol.* 10, 383 **(2014)**.

225. Y. Celina, N. Mehrnoosh, V. P. Monique, and B. C. Devika, Cancer nanotechnology: Enhanced therapeutic response using peptide-modified gold nanoparticles. *J. Nanosci. Nanotechnol.* 14, 4813 **(2014)**.

226. J. Xie, G. Liu, H. S. Eden, H. Ai, and X. Chen, Surface-engineered magnetic nanoparticle platforms for cancer imaging and therapy. *Acc Chem. Res.* 44, 883 **(2011)**.

227. C. Tassa, S. Y. Shaw, and R. Weissleder, Dextran-coated iron oxide nanoparticles: A versatile platform for targeted molecular imaging, molecular diagnostics, and therapy. *Acc Chem. Res.* 44, 842 **(2011)**.

228. D. Peer, J. M. Karp, S. Hong, O. C. Farokhzad, R. Margalit, and R. Langer, Nanocarriers as an emerging platform for cancer therapy. *Nat. Nanotechnol.* 2, 751 **(2007)**.

229. F. M. Kievit and M. Zhang, Surface engineering of iron oxide nanoparticles for targeted cancer therapy. *Acc Chem. Res.* 44, 853 **(2011)**.

230. D. A. Giljohann and C. A. Mirkin, Drivers of biodiagnostic development. *Nature* 462, 461 **(2009)**.

231. C. Sun, K. Du, C. Fang, N. Bhattarai, O. Veiseh, F. Kievit, Z. Stephen, D. Lee, R. G. Ellenbogen, and B. Ratner, PEG-mediated synthesis of highly dispersive multifunctional superparamagnetic nanoparticles: Their physicochemical properties and function *in vivo*. *ACS Nano* 4, 2402 **(2010)**.

232. E. Ruiz-Hernandez, A. Baeza, and M. Ü. Vallet-Regilü, Smart drug delivery through DNA/magnetic nanoparticle gates. *ACS Nano* 5, 1259 **(2011)**.

233. B. Kim, G. Han, B. J. Toley, C. k. Kim, V. M. Rotello, and N. S. Forbes, Tuning payload delivery in tumour cylindroids using gold nanoparticles. *Nat. Nanotechnol.* 5, 465 **(2010)**.

234. F. M. Kievit, O. Veiseh, C. Fang, N. Bhattarai, D. Lee, R. G. Ellenbogen, and M. Zhang, Chlorotoxin labeled magnetic nanovectors for targeted gene delivery to glioma. *ACS Nano* 4, 4587 **(2010)**.

235. B. P. Barnett, A. Arepally, P. V. Karmarkar, D. Qian, W. D. Gilson, P. Walczak, V. Howland, L. Lawler, C. Lauzon, and M. Stuber, Magnetic resonance-guided, real-time targeted delivery and imaging of magnetocapsules immunoprotecting pancreatic islet cells. *Nat. Med.* 13, 986 **(2007)**.

236. O. T. Bruns, H. Ittrich, K. Peldschus, M. G. Kaul, U. I. Tromsdorf, J. Lauterwasser, M. S. Nikolic, B. Mollwitz, M. Merkel, and N. C. Bigall, Real-time magnetic resonance imaging and quantification of lipoprotein metabolism *in vivo* using nanocrystals. *Nat. Nanotechnol.* 4, 193 **(2009)**.

237. A. L. Miranda-Vilela, R. C. Peixoto, J. P. Longo, F. A. Portilho, K. L. Miranda, P. P. Sartoratto, S. N. Bao, R. B. de Azevedo, and Z. G. Lacava, Dextran-functionalized magnetic fluid mediating magnetohyperthermia combined with preventive antioxidant pequi-oil supplementation: Potential use against cancer. *J. Biomed. Nanotechnol.* 9, 1261 **(2013)**.

238. C. J. Meledandri, J. K. Stolarczyk, and D. F. Brougham, Hierarchical gold-decorated magnetic nanoparticle clusters with controlled size. *ACS Nano* 5, 1747 **(2011)**.

239. L. Hirsch, R. J. Stafford, J. A. Bankson, S. R. Sershen, B. Rivera, R. E. Price, J. D. Hazle, N. J. Halas, and J. L. West, Nanoshell-mediated near-infrared thermal therapy of tumors under magnetic resonance guidance. *Proc. Natl. Acad. Sci.* 100, 13549 **(2003)**.

240. L. Wang, J. Bai, Y. Li, and Y. Huang, Multifunctional nanoparticles displaying magnetization and near-IR absorption. *Angew. Chem. Int. Ed.* 47, 2439 **(2008)**.

241. S. Guo, S. Dong, and E. Wang, A general route to construct diverse multifunctional Fe_3O_4/metal hybrid nanostructures. *Chem. Eur. J.* 15, 2416 **(2009)**.

242. J. Kim, S. Park, J. E. Lee, S. M. Jin, J. H. Lee, I. S. Lee, I. Yang, J.-S. Kim, S. K. Kim, and M.-H. Cho, Designed fabrication of multifunctional magnetic gold nanoshells and their application to magnetic resonance imaging and photothermal therapy. *Angew. Chem.* 118, 7918 **(2006)**.

243. Z. Fan, M. Shelton, A. K. Singh, D. Senapati, S. A. Khan, and P. C. Ray, Multifunctional plasmonic shell-magnetic core nanoparticles for targeted diagnostics, isolation, and photothermal destruction of tumor cells. *ACS Nano* 6, 1065 **(2012)**.

244. M. Famulok, J. S. Hartig, and G. Mayer, Functional aptamers and aptazymes in biotechnology, diagnostics, and therapy. *Chem. Rev.* 107, 3715 **(2007)**.

245. W. C. Huang, P. J. Tsai, and Y. C. Chen, Multifunctional Fe_3O_4@ Au nanoeggs as photothermal agents for selective killing of nosocomial and antibiotic-resistant bacteria. *Small* 5, 51 **(2009)**.

246. J. Ren, S. Shen, Z. Pang, X. Lu, C. Deng, and X. Jiang, Facile synthesis of superparamagnetic Fe_3O_4@ Au nanoparticles for photothermal destruction of cancer cells. *Chem. Commun.* 47, 11692 **(2011)**.